AD-A039 797 NAVAL POSTGRADUATE SCHOOL MONTEREY CALIF F/G 20/6

POWER-DENSITY DISTRIBUTION BELOW THE OCEAN SURFACE DUE TO INCID--ETC(U)

MAR 77 M J MILCHANOWSKI

UNCLASSIFIED NL

1 OF 1

AD A039797

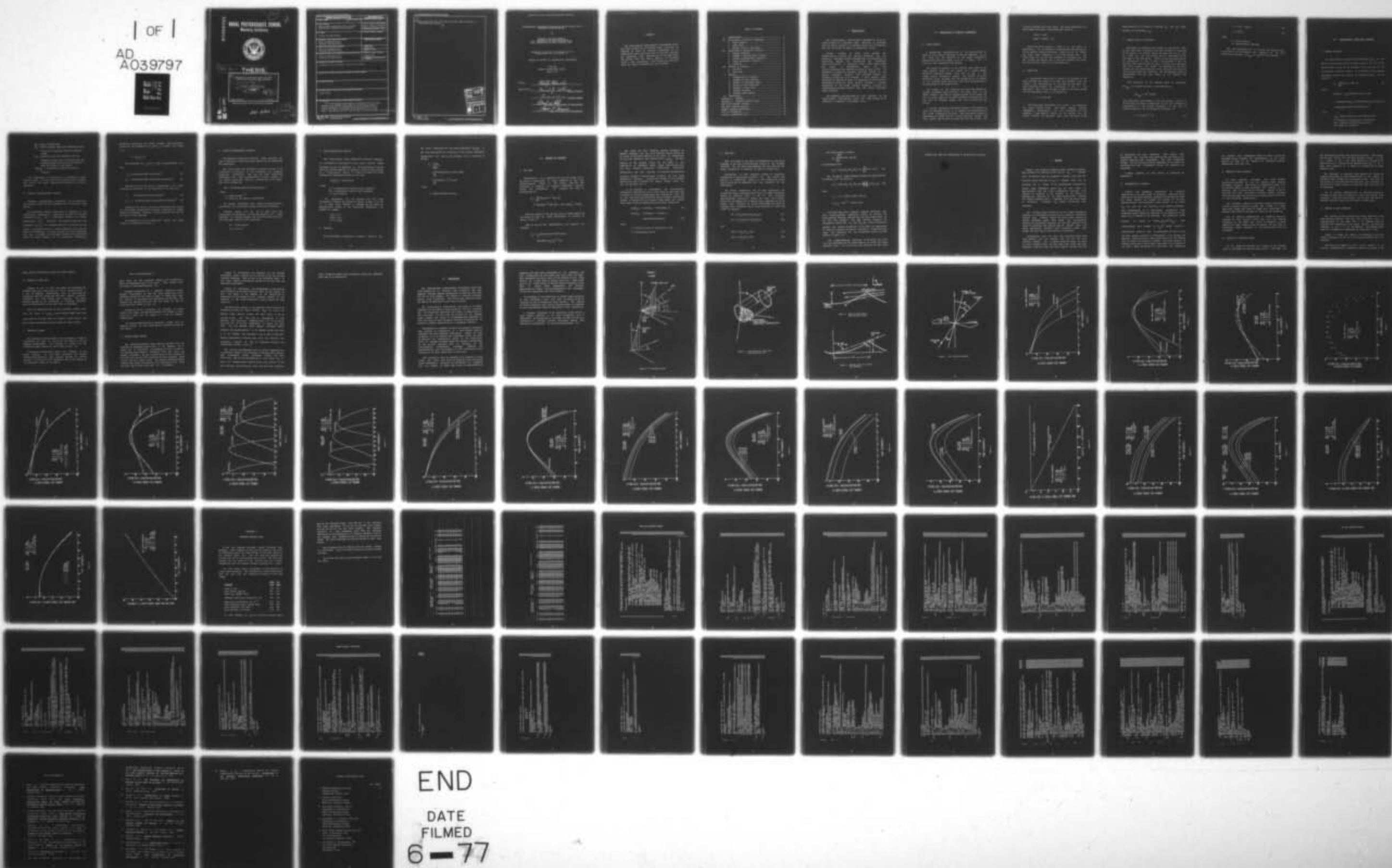

END

DATE FILMED

6-77

ADA039797

NAVAL POSTGRADUATE SCHOOL

Monterey, California

9 Master's THESIS

6 POWER-DENSITY DISTRIBUTION BELOW THE OCEAN SURFACE DUE TO INCIDENT LASER RADIATION

by

10 Michael John Milchanowski

11 Mar[redacted]977

12 85p.

Thesis Advisor: D. J. Collins

Approved for public release; distribution unlimited.

DDC
RECEIVED
MAY 24 1977
A

AD No.
DDC FILE COPY

251 450

SECURITY CLASSIFICATION OF THIS PAGE (When Data Entered)

REPORT DOCUMENTATION PAGE		READ INSTRUCTIONS BEFORE COMPLETING FORM
1. REPORT NUMBER	2. GOVT ACCESSION NO.	3. RECIPIENT'S CATALOG NUMBER
4. TITLE (and Subtitle) POWER-DENSITY DISTRIBUTION BELOW THE OCEAN SURFACE DUE TO INCIDENT LASER RADIATION		5. TYPE OF REPORT & PERIOD COVERED Master's Thesis; (March 1977)
		6. PERFORMING ORG. REPORT NUMBER
7. AUTHOR(s) Michael John Milchanowski		8. CONTRACT OR GRANT NUMBER(s)
9. PERFORMING ORGANIZATION NAME AND ADDRESS Naval Postgraduate School Monterey, California 93940		10. PROGRAM ELEMENT, PROJECT, TASK AREA & WORK UNIT NUMBERS
11. CONTROLLING OFFICE NAME AND ADDRESS Naval Postgraduate School Monterey, California 93940		12. REPORT DATE March 1977
		13. NUMBER OF PAGES 85
14. MONITORING AGENCY NAME & ADDRESS(if different from Controlling Office) Naval Postgraduate School Monterey, California 93940		15. SECURITY CLASS. (of this report) Unclassified
		15a. DECLASSIFICATION/DOWNGRADING SCHEDULE

16. DISTRIBUTION STATEMENT (of this Report)

Approved for public release; distribution unlimited.

17. DISTRIBUTION STATEMENT (of the abstract entered in Block 20, if different from Report)

18. SUPPLEMENTARY NOTES

19. KEY WORDS (Continue on reverse side if necessary and identify by block number)

Laser, Ocean

20. ABSTRACT (Continue on reverse side if necessary and identify by block number)

The time-averaged power-density distribution below the ocean surface due to incident laser radiation is examined by means of computer simulation of the geometrical optics involved with the air/sea interface and subsequent ocean penetration by the laser beam. The effects over the entire spectra of incidence angles, → next page

DD FORM 1 JAN 73 1473 EDITION OF 1 NOV 65 IS OBSOLETE
(Page 1) S/N 0102-014-6601 |

SECURITY CLASSIFICATION OF THIS PAGE (When Data Entered)

cont

wind velocities, wind directions, beam spot sizes and depths of penetration are analyzed.

White Section
Buff Section
UNANNOUNCED
JUSTIFICATION
BY
DISTRIBUTION/AVAILABILITY CODES
Dist. AVAIL. and/or SPECIAL

Approved for public release; distribution unlimited.

POWER-DENSITY DISTRIBUTION BELOW THE OCEAN SURFACE DUE TO INCIDENT LASER RADIATION

by

Michael John Milchanowski
Lieutenant, United States Navy
B.S., United States Naval Academy, 1969
M.S., University of West Florida, 1971

Submitted in partial fulfillment of the requirements for the degree of

MASTER OF SCIENCE IN AERONAUTICAL ENGINEERING

from the

NAVAL POSTGRADUATE SCHOOL

March 1977

Author: Michael John Milchanowski

Approved by: Daniel J. Collins, Thesis Advisor

Theodore H. Gawain, Second Reader

Richard W. Bell, Chairman, Department of Aeronautics

Robert R. Fossum, Dean of Science and Engineering

ABSTRACT

The time-averaged power-density distribution below the ocean surface due to incident laser radiation is examined by means of computer simulation of the geometrical optics involved with the air/sea interface and subsequent ocean penetration by the laser beam. The effects over the entire spectra of incidence angles, wind velocities, wind directions, beam spot sizes and depths of penetration are analyzed.

TABLE OF CONTENTS

I. INTRODUCTION

The time-averaged power-density distribution below the ocean surface due to incident laser radiation is examined over the entire spectra of incidence angles, wind velocities and wind directions by means of geometrical optics.

Current interest in using laser systems for communications through the air-sea interface and for detecting submerged objects necessitates the development of prediction methods for determining the subsurface power-distribution of radiation from a laser source above the ocean. A mathematical model for the optical-communications application done by Karp in Ref. 1 is developed in terms of a radiance function related to the mutual coherence function with accurate results for incidence angles out to 45 degrees. A more general model developed by Swennen in Refs. 2-4 examines the power-density distribution below the ocean surface through a rigorous assessment of the ocean surface geometry allowing for theoretically accurate results over the entire incidence angle spectrum.

The computer code developed for this analysis of the power-density distribution below the ocean surface is an expansion of Swennen's theory[Refs. 2-4].

II. DESCRIPTION OF PHYSICAL PARAMETERS

A. OCEAN SURFACE

A geometrical representation of the ocean surface in terms of local slopes developed by Cox and Munk[Ref. 5] is the basis for the analysis of the power probability distribution below the ocean, as it is in Refs. 2-4. A review of this representation follows.

The center of symmetry of the incident laser beam on the ocean surface facet is the center of a right- handed cartesian coordinate system, point "O" in Fig. 1. The z-axis points vertically upward. The y-axis is in the horizontal plane, colinear with the projection of the center of the incident laser beam onto that plane and pointing in the direction of the laser source.

The slopes of the ocean surface facet are defined by angular parameters Alpha and Beta. The angle Beta is the angle between the line of steepest ascent of the facet and the x-y plane; Alpha is the angle between the projection of the line of steepest ascent onto the x-y plane and the y-axis.

A second cartesian coordinate system at the surface is used, as explained in Ref. 2, to simplify the computation of the slope probability function. This coordinate system is designated by primes with the y'-axis pointing towards the wind source and rotated an angle Chi from the y-axis. The

z'-axis coincides with the z-axis. The slope parameters are also primed with their transformations given by:

Beta' = Beta

Alpha' = Alpha - Chi

Below the ocean surface a depth Z at the point of observation, O', is centered a translational transformation of the surface coordinate system. Angles Mu and Nu define the laser beam refracted to O' by any surface facet. The first angle, Mu, is the angle between the refracted ray and the z-axis; the second, Nu, is the angle between the y-axis and the vertical plane of the refracted ray.

B. LASER BEAM

A cylindrical laser beam of radius a is incident on the ocean surface wave facet at an angle Psi measured from the z-axis. The intersection of the beam and the facet is a flat elliptical surface as illustrated in Fig. 2. The semi-minor axis of the ellipse is equal to the beam radius and the semi-major axis, b, is defined by:

b = a * sec Psi

The analytical development, as in Refs. 2-4, begins at the ocean surface facet. The laser source, aiming, atmospheric propagation, etc. are extraneous to this analysis. Power density values at the surface are not quoted because the analysis deals with the ratio of the

power density at the depth of interest, P_d, and the power density at the surface, P_{ds}.

C. MAXIMUM ANGLE OF INCIDENCE

The angle of incidence with respect to the z-axis, Psi, of the laser beam is analyzed from zero degrees to a maximum of 84 degrees. At greater angles the beam will not be able to strike all the wave facets within a wavelength of the wave due to the wave height. There is also the possibility, as illustrated in Fig. 3, that a ray incident at Psi > 84 degrees could pass through the wave, re-enter the atmosphere and then re-enter the ocean; or, depending on the local slopes, the ray could undergo a total internal reflection if the Critical Angle were exceeded. The mathematical model of Swennen[Refs. 2-4] and this thesis do not address this situation.

This limitation on the maximum angle of incidence, Psi_{max}, is derived from Fig. 4 and defined by:

$$Psi_{max} = \tan^{-1}(L/2H)$$

The significant wave height, H, and the average period, T, of the wave are given by equations (1) and (2) as defined by Pierson[Ref. 7]. The average wavelength of the wave is given by equation (3) as defined by Hill[Ref. 8].

$$H = 2.14x10^{-2} * W^2 \qquad (1)$$

$$T = 0.81 * (2W/g) \quad (2)$$

$$L = gT^2/2 \quad (3)$$

where

W = wind velocity

g = gravitational constant

For wind velocities of 1 to 14 m/sec the maximum angle of incidence is 84.2 degrees (±0.4 degrees) for all wind velocities; therefore, Psi_{max} is limited to 84 degrees.

III. POWER-DENSITY PROABILITY INTEGRAL

A. GENERAL EQUATION

The power-density probability distribution (P_d) at the point of observation below the ocean surface (O') due to the entire beam is given by the integral of dP_d over all of the contributing surface facets. As a function of the angular parameters (Mu,Nu) the integral as defined in Refs. 2-4 is given by:

$$P_d = \int_{\mu}\int_{\nu} F(Mu,Nu)\ dMu\ dNu \qquad (4)$$

where

$$F(Mu,Nu) = P_{ds}*T*DTF*\cos(WI)*\sec(WR)$$

$$*[\cos(Mu)*\cos(Mu_0)+\sin(Mu)*\sin(Mu_0)*\cos|Nu-Nu_0|]$$

$$*P(Z'_x,Z'_y)*\tan(Beta)*\sec^2(Beta)*J^{-1}$$

and

P_{ds} = power density at the surface facet

T = Fresnel's transmittance coefficient

DTF = diffuse transmittance function

WI = angle of incidence

WR = angle of refraction

Mu_0 = first quadrant angle the refracted center ray of the beam makes with the positive z-axis

Nu_0 = positive angle the projection of the refracted center ray of the beam onto the xy-plane makes with the y-axis measured from the latter to the former

$P(Z'_x, Z'_y)$ = time-average slope distribution function

The development of equation (4) is described in great detail in Refs. 2-4 and will not be repeated here; however, for clarity the major components of equation (4) will be discussed.

B. FRESNEL'S TRANSMITTANCE FUNCTION

Fresnel's transmittance coefficient (T) is defined as the intensity ratio of the transmitted to the incident beam energy.

The collimated incident laser beam is composed of two polarization components, a transverse magnetic or parallel polarization ($T_{//}$) and a transverse electric or normal polarization ($T_{\perp}$). Resolving the refracted beam into its components ($T_{\perp}, T_{//}$) is a complex task due to rotation of the plane of incidence about all three coordinate axis over the range of integration. In order to deal with this complexity the beam is assumed to be rendered diffuse and unpolarized below the ocean surface due to scattering, propagation

direction variations and phase changes. This assumption allows for the averaging of $T_{\perp}$ and $T_{//}$ to obtain the value of T.

$$T = (T_{\perp} + T_{//})/2$$

The equations for $T_{\perp}$ and $T_{//}$ used by Swennen[Refs. 2-4] are:

$$T_{\perp} = [\sin(WI)*\sin(WR)/\sin(WI+WR)]^2 \quad (5)$$

$$T_{//} = [\sin(WI)*\sin(WR)/\sin(WI+WR)*\cos(WI-WR)]^2 \quad (6)$$

Equations (5) and (6) are in disagreement with those developed by Born[Ref. 9] and Fowles[Ref. 10], given by:

$$T_{\perp} = [2*\cos(WI)*\sin(WR)/\sin(WI+WR)]^2 \quad (7)$$

$$T_{//} = [2*\cos(WI)*\sin(WR)//\sin(WI+WR)*\cos(WI-WR)]^2 \quad (8)$$

Equations (5) and (6) will give erroneously high values for the Fresnel transmittance function, especially at higher angles of incidence. Because of this, equations (7) and (8) are used in this modeling.

The geometry of the ray refraction through the ocean surface is illustrated in Fig. 5.

C. DIFFUSE TRANSMITTANCE FUNCTION

The diffuse transmittance function (DTF) accounts for beam attenuation below the ocean surface due to scattering and absorbticn.

The six-constant DTF developed by Duntley in Ref. 11 is simplified tc a function of two constants; the backward scattering coefficient (BS) and the total absorbtion coefficient (AC). This simplification is valid because of the randcm scattering particle orientation in the ocean. The DTF is defined by:

DTF = K/[(AC+BS)*sinh(K*Z)+K*cosh(K*Z)]

where

$K = [AC*(AC+2BS)]^{1/2}$

Z = depth of the point of observation

In current terminolgy this method of accounting for attenuaticn is a zero-angle forward scattering technique.

Typical values for BS and AC were used from measurements by Tyler[Ref. 12] and Duntley[Ref. 13]. These represent an average between cool and warm ocean waters in the blue-green spectrum (4800 angstrom).

BS = 0.065 percent

$AC = 0.044\ m^{-1}$

D. SLOPE PROBABILITY FUNCTION

The time-average slope probability function, $P(Z'_x, Z'_y)$, is a statistical distribution of the ocean surface slopes developed by Cox and Munk[Ref. 5]. The distribution derived from the surface geometry is Gaussian, which is then altered by a Gram-Charlier series in order to account for slope skewness and peakedness caused by the wind.

$$P(Z'_x, Z'_y) = f(Xi, Eta, W)$$

where

Xi = standardized crosswind slope component

Eta = standardized upwind slope component

W = wind velocity

The development and the equation for the slope probability function are covered in detail in Refs. 2,4, and 5. A clean ocean surface is assumed and the limits of applicability placed on the functional parameters are adhered to, namely:

$$|Xi| \le 2.5$$
$$|Eta| \le 2.5$$
$$W \le 14 \text{ m/sec}$$

E. JACOBIAN

The power-density probability integral, equation (4),

was first developed over the slope components (Z'_x, Z'_y). It was then transformed to a function of the angular parameters (Alpha,Beta) and then by the Jacobian (J) to a function of (Mu,Nu).

$$P_d = \iint_{Z'_x Z'_y} dP_d$$

$$= \iint_{\alpha\,\beta} F(\text{Alpha},\text{Beta})\ d\text{Alpha}\ d\text{Beta}$$

$$= \iint_{\mu\,\nu} F(\text{Mu},\text{Nu})\ J^{-1}\ d\text{Mu}\ d\text{Nu}$$

where

$$J = \partial(\text{Mu},\text{Nu})/\partial(\text{Alpha},\text{Beta})$$

IV. METHODS OF SOLUTION

A. FAR ZONE

Swennen[Refs. 2-4] observed that when the depth (Z) of the point of observation is large compared to the beam cross-sectional radius at the surface (Z/a>100) the integrand of equation (4) remains essentially constant during the integration. The integral can then be approximated by:

$$P_d = \iint_{\mu\, \nu} F(Mu,Nu)*J^{-1}\ dMu\ dNu$$

$$\simeq F(Mu,Nu)*J^{-1}\ \Delta Mu\ \Delta Nu\ ;\ \text{with } Mu=Mu_0\ \&\ Nu=Nu_0$$

The area $\Delta Mu \Delta Nu$ in the (Mu,Nu) plane is approximated by an ellipse of area ΔA, whose development is covered in detail in Ref. 3.

This is the Far Zone approximation and equation (4) becomes:

$$P_d = P_{ds}*T*\tan(Beta)*\sec^2*\cos(WI)$$

$$*\sec(WR)*P(Z'_x,P'_y)*J^{-1}*\Delta A$$

The basic Far Zone computer program developed in FORTRAN language and run on the IBM 360 system solves for the ratio of the power density at the point of observation to the power density at the surface facet, P_d/P_{ds}. The main portion of the program allows for the entry of any combination of variables (wind, depth, beam radius, Psi, Chi, Nu_0, backward scattering coefficient, absorbtion coefficient), and also computes the diffuse transmittance function, Fresnsl's transmittance function and the slope probability function. Subroutines common to all variable entries are used to compute the angles (Alpha, Beta, WI, WR), the Jaccbian and A.

It is possible to investigate the power-density probability distribution over a wide range of variables with a minimal of storage requirements and computation time due to the use of an IBM System/360 Source Library subroutine, NLNSYS, in solving for the coupled (Alpha,Beta) and (Mu,Nu) angle pairs from the simultaneous non-linear equations:

$$\cos(Mu_0) = [\cos(Psi) + K*\cos(Beta)]/n \qquad (9)$$

$$\cot(Nu_0) = \cot(Alpha) - \sin(Psi)/K *\sin(Alpha)*\sin(Beta) \qquad (10)$$

where

n = relative index of refraction (1.33)

K = K(Psi,Alpha,Beta,n)

B. NEAR ZONE

When the depth of the point of observation is not large compared to the beam cross-sectional radius at the surface ($Z/a<100$) the Far Zone approximation does not hold and the double integration of equation (4) must be carried out.

Swennen[Ref. 2] used Simpson's method of numerical integration to approximate equation (4). The method was subject to singularity points in the integration limits which increased the complexity and time required for the computation.

The double integration can be more accurately and relatively simply approximated by using the Gauss Quadrature system of solution, Refs. 14 and 15. The Two-Point Gauss-Legendre Quadrature method was used. This method, valid for polynomials up to degree three (equation (4) is of degree two), consists of first transforming the function F(Mu,Nu) into a function F(s,t) whose interval is $-1\leq s\leq 1$ and $-1\leq t\leq 1$ by letting:

$$Mu = [(Mu_u - Mu_l)*s + Mu_u + Mu_l]/2 \tag{11}$$

$$Nu = [(Nu_u - Nu_l)*t + Nu_u + Nu_l]/2 \tag{12}$$

and

$$dMu = [(Mu_u - Mu_l)/2]ds \tag{13}$$

$$dNu = [(Nu_u - Nu_l)/2]dt \tag{14}$$

The power-density integral

$$P_d = \int_{\mu_l}^{\mu_u}\int_{\nu_l}^{\nu_u} F(Mu,Nu)\ dMu\ dNu$$

is transformed into

$$P_d = [(Mu_u - Mu_l)(Nu_u - Nu_l)/4]*\int_{-1}^{1}\int_{-1}^{1} F(s,t)\ ds\ dt \qquad (15)$$

The Two-Point Gauss-Legendre Quadrature approximation of equation (13) is given by:

$$P_d = [(Mu_u - Mu_l)(Nu_u - Nu_l)/4]*\sum_{i=0}^{1}\sum_{j=0}^{1} W_i * F(s_i, t_j) \qquad (16)$$

where

$$W_i = 1.0 = \text{Gauss weight factors}$$

$$s_i, t_j = \pm(3)^{-2} = \text{Gauss roots}$$

The basic Near Zone computer program developed uses this Gauss-Legendre Quadrature method in solving the power-density integral coupled with the same subroutines as the Far Zone program. The main program computes the integration limits (Mu_u, Mu_l) and (Nu_u, Nu_l) after determining whether the surface projection of the point of observation is inside or outside the beam's horizontal cross-sectional area. The equations for the integration limits are well defined in Refs. 2-4.

The transformations described by equations (11)-(15) are then performed and the power-density is solved for using equation (16). As in the Far Zone program, the Near Zone

program can take any combination of variables as entries.

V. RESULTS

Results for oblique incidence angles ($0<Psi\leq84$ degrees) were obtained for vertical plane cuts at $Nu_0 = 0$ degrees over the entire range of variables; however, valid data for vertical planar sections at $Nu_0 \neq 0$ degrees could not be obtained due to values of the standardized crosswind and upwind slope components being out of the range of applicability for the slope probability function. This problem is believed to be inherent in the method of mathematical analysis of the ocean surface used. Results for normal incidence (Psi = 0 degrees) over the entire range of variables, including Nu_0 planar variations, were obtained.

The validity check carried out on the slope probability function, as discussed in Section III.D, clearly identified invalid data. Another source of invalid data occurred at higher incidence angles (Psi) where the simultaneous solution of non-linear equations (9) and (10) resulted in an angle of incidence (WI) greater than 90 degrees while the slope probability function still indicated valid. This output was also easily identified and eliminated.

Computations with the Near Zone solution method used more computer time and storage than did the Far Zone solution method. For a computer solution using one value for each variable entry, the Near Zone used 36 per cent more computer time and 8 per cent more computer storage than did

an equivalent Far Zone solution. The higher time requirement for the Near Zone solution was due mainly to a greater compiling time requirement. The time difference between the two solution methods decreased as the number of variables that were incremented during one computer run increased.

A sample computer run with output is presented in Appendix B.

A. PRESENTATION OF RESULTS

Results are presented graphically to simplify comparisons of the wide range of variables. Vertical-planar sections of the power density probability distribution below the ocean surface cut through the center of the beam cross-section at the horizontal ocean surface at an angle Nu_0 are used for the majority of the results presented. This presentation is in rectangular coordinates with normalized power density in decibels on the ordinate and the angle Mu_0 in degrees on the abscissa. The normalized power density is equal to $10*\log_{10}[(P_d*Z^2)/P_{ds}]$. This normalization with respect to P_{ds}/Z^2 should produce a distribution function that is independent of depth in the Far Zone regime, according to Swennen[Ref. 2-4], because the multiple slopes seen in a beam cross-section at the surface tend to render the radiation diffuse. The power density of diffuse radiation at large depths decreases as the square of the depth. When the effects of scattering and absorption

are included this independence does not occur, as will be discussed later; however, the normalization of the power density is used in all regimes for continuity and for comparisons with Refs. 2-4.

B. EFFECTS OF WIND VELOCITY

As wind velocity increases, the power density distribution spreads out and the maximum power density decreases slightly. This effect is presented in Figs. 6-11 for various angles of beam incidence with respect to the vertical (Psi = 0,30,60 and 84 degrees). Figures 10 and 11 also show the close correlation between results obtained from the Near Zone and the Far Zone solution methods for Psi = 0 and 40 degrees, respectively.

The spreading effect on the power density distribution is due to larger refraction angles (WR) caused by higher wave facet slopes that occur at higher wind velocities. The maximum power density decrease is caused by the spreading.

For an optical communication or detection system an increase in wind velocity would mean that the maximum intensity of the beam that could be focused to a point beneath the ocean surface would be reduced, but the width of receivable signal radiation or the search width would be increased.

C. EFFECTS OF INCIDENCE ANGLE

As the angle of incidence with respect to the vertical (Psi) is increased the maximum power density decreases and

the distribution shifts away from the vertical. This effect can be seen in Figs. 6-11 and more clearly in Figs. 12 and 13. Figure 12 is a Far Zone solution at a depth of 50 meters for Psi = 0,30,60 and 84 degrees while Fig. 13 is a Near Zone solution at a depth of 10 meters for the same values of Psi.

The decrease in maximum power density is a result of greater reflectance at the surface facet as the angles of incidence (WI) increase with increases in Psi. The shift in the center of the distributions away from the vertical is caused by the higher angles of refraction (WR) that occur as WI increases.

For an optical communication or detection system an increase in Psi would be expected to lower the maximum beam intensity below the ocean surface and to shift the point of maximum intensity away from the point of water entry.

D. EFFECTS OF WIND DIRECTION

The effects of wind direction are small compared to the wind velocity effects. When the wind direction (Chi) is perpendicular to the beam (Chi = 90 degrees) there is slightly less spreading of the power density distribution compared to Chi = 0 or 180 degrees. The maximum power density is essentially unaffected by variations in Chi.

Figure 14 shows the effect of variations in Chi for normal incidence and Fig. 15 for oblique incidence (Psi = 40 degrees).

Wind direction appears to be of little concern to an optical communication or detection system as related to the

power density distribution below the ocean surface.

E. EFFECTS OF SPOT SIZE

Figures 16 and 17 show the effect of increasing the incident beam spot radius from 0.1 to 0.5 meters for Psi = 0 and 40 degrees, respectively. This is done with the assumption that the energy per unit area remains constant; therefore, the total energy must increase. The power density spreads out and increases in intensity uniformly over the distribution as the spot size is increased.

Since the equations used in this solution method deal with the ratio of P_d/P_{ds}, these results simply mean that more power in a larger beam will produce a more intense and more widely distributed pattern below the ocean surface.

F. EFFECTS OF DEPTH

The decrease of power density with increases in depth is illustrated in Figs. 18 and 19 for Psi equal to 0 and 40 degrees, respectively. The decrease is linear for the normalized power density as can be seen in Fig. 20.

Scattering and absorption cause this decrease in the power density. As the depth increases the diffuse transmittance function (DTF) rapidly becomes an inverse function of the sum of the hyperbolic sine of the depth and the hyperbolic cosine of the depth,

$$DTF = f[(\sinh Z+\cosh Z)^{-1}]$$

which means the DTF decreases rapidly with increases in depth and approaches zero in the limit. This agrees with the theory of Preisendorfer[Ref. 16].

Swennen's prediction of a constant normalized power density distribution in the Far Zone regime due to the diffusing effects of the ocean in Refs. 2-4 holds only when the effects of scattering and absorption are ignored. One computer run was made with the DTF set equal to one to illustrate this effect in Fig. 20.

Figures 21 and 22 illustrate the decrease in power density with depth, non-dimensionalized with respect to spot size, Z/a, again for Psi equal to 0 and 40 degrees, respectively.

An optical communication or detection system will be limited greatly by the power density decrease associated with depth.

G. MAXIMUM POWER DENSITY

The maximum obtainable power density available over the spectrum of incidence angles (Psi = 0 - 84 degrees) for a given set of conditions is presented in Figs. 23 and 24. The maximum power density obtainable does not occur for normal incidence, but for a small value of Psi, because of the fact that as the wind increases the most probable slope is not zero but a small angle. The maximum obtainable power density then drops continuously with increases in Psi after the peak that occurs around Psi = 10 - 15 degrees.

Figure 23 illustrates the decrease in the maximum obtainable power density for all values of Psi as the wind velocity increases. This is due to the spreading effect on the power density distribution caused by the wind that was described previously.

Figure 24 illustrates the independence of the maximum power density on the wind direction (Chi) for all values of Psi. Chi equal to 270 degrees is not plotted but is equivalent to the condition at 90 degrees because of the symmetry of the slope probability function about the wind direction.

The angle with respect to the vertical from the point of observation below the ocean surface (Mu_0) at which the maximum power density occurs for each value of Psi is plotted in Fig. 25. The plot is independent of wind velocity and direction. Examining Figs. 16 - 19 it can be seen that Fig. 25 is also independent of depth and spot size. Mu_0 for maximum power density increases nearly linearly from approximately 1 to 56 degrees as Psi goes from 0 to 84 degrees. The increase in Mu_0 is due to the power density distribution shifting away from the vertical for increasing valules of Psi as discussed earlier and illustrated in Figs. 12 and 13.

The obvious consideration with an optical communication or detection system is the decrease in maximum power density that accompanies higher incidence angles and wind velocities. The strong independence of the angle Mu_0 at which the maximum power density occurs with respect to the wind velocity, wind direction, depth and spot size indicates

that a satellite based laser navigation system for submarine usage may be a possibility.

VI. CONCLUSIONS

The time-averaged power-density distribution below the ocean surface due to incident laser radiation has been examined through computer simulations in both the Near Zone and the Far Zone regimes. The effects of altering incidence angles, wind velocities, wind directions, beam spot sizes and depths of penetration have been presented.

The power-density distribution was found to be highly dependent on the angle of beam incidence, the wind velocity and the attenuation associated with depth of penetration of the laser beam. The fact that the location of the maximum power density was found to be fundamentally dependent on only the angle of beam incidence indicates a possibility of direction finding capabilities by a submerged receiver.

Improvements in computer systems and analysis techniques have allowed an examination of a much broader range of variables than were possible heretofore. Angles of beam incidence up to 84 degrees were considered within the range of validity for restrictions placed on the simulation. Above 84 degrees incidence angle the possible interactions at the air/sea interface make an analysis of the power-density distribution extremely complex, and experimentation will be necessary to give indications of the feasibility of laser operations in this area.

This simulation could be extended to an analysis of much larger spot sizes that would be expected from a satellite based transmitter. Prettyman and Cermak[Ref. 17] suggested that the effects of larger spots could be approximated by

assuming each wave facet independent of its neighbors and then integrating over the larger spot area, since the small spot represents the outer limit of the effects of the ocean surface on a laser beam of greater spot size. There would have to be a large number of surface facets contained in the spot to insure facet independence and accurate approximations, hence a strong dependence on the wavelength of the wave associated with wind velocity.

An extension of the simulation to pulsed laser radiation is also warrented, since this mode of operation may be required for air-to-subsurface laser systems. The effects of pulsed radiation occur nearly instantaneously as compared to the time-averaged analysis performed in this simulation.

A further refinement of the simulation would involve a more complex modeling of the beam attenuation due to scattering and absorption in the ocean through the use of a diffusion or a multiple forward scattering method, both described by Bucher[Ref. 18] and Preisendorfer[Ref. 16].

APPENDIX A

FIGURES

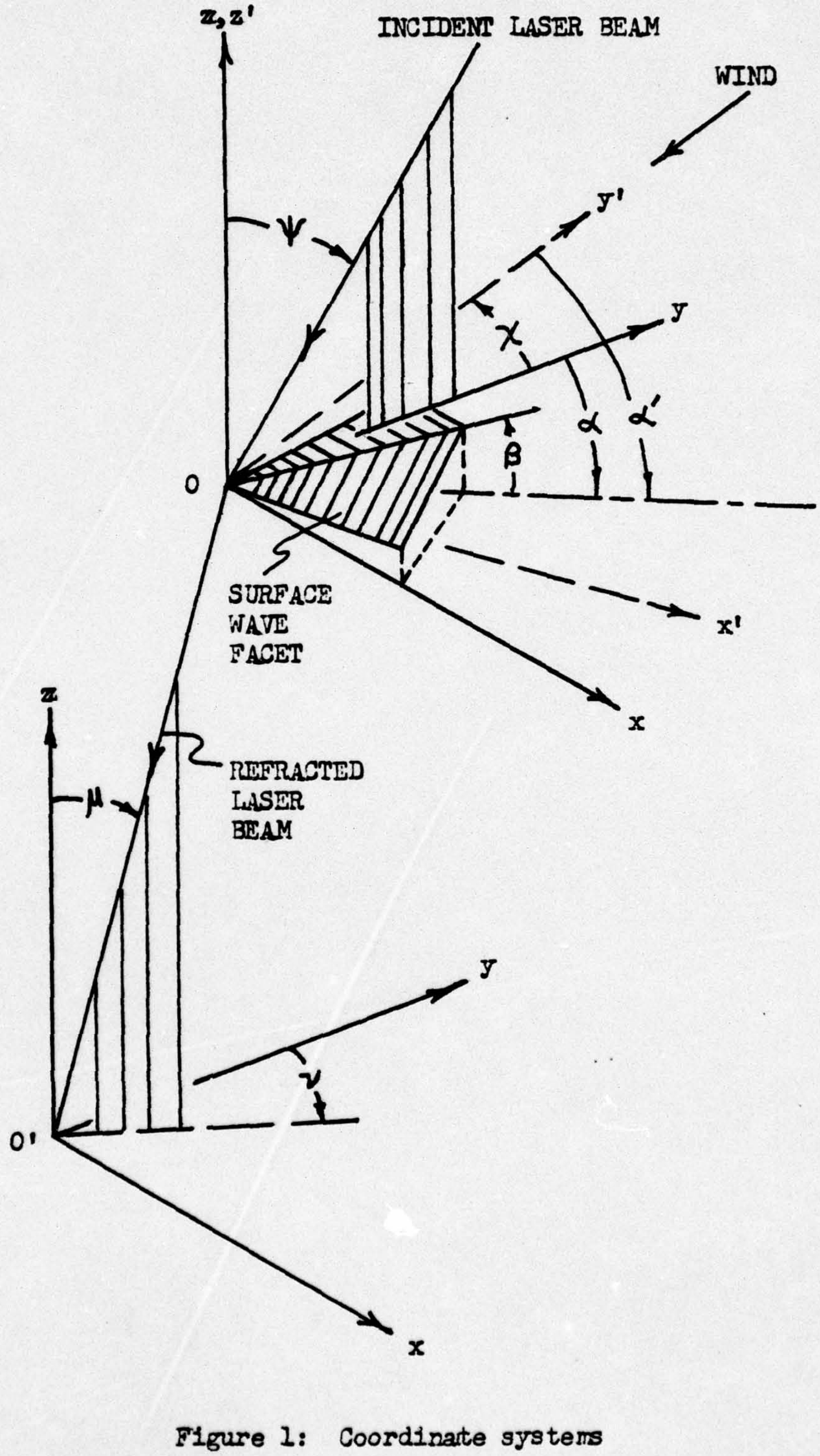

Figure 1: Coordinate systems

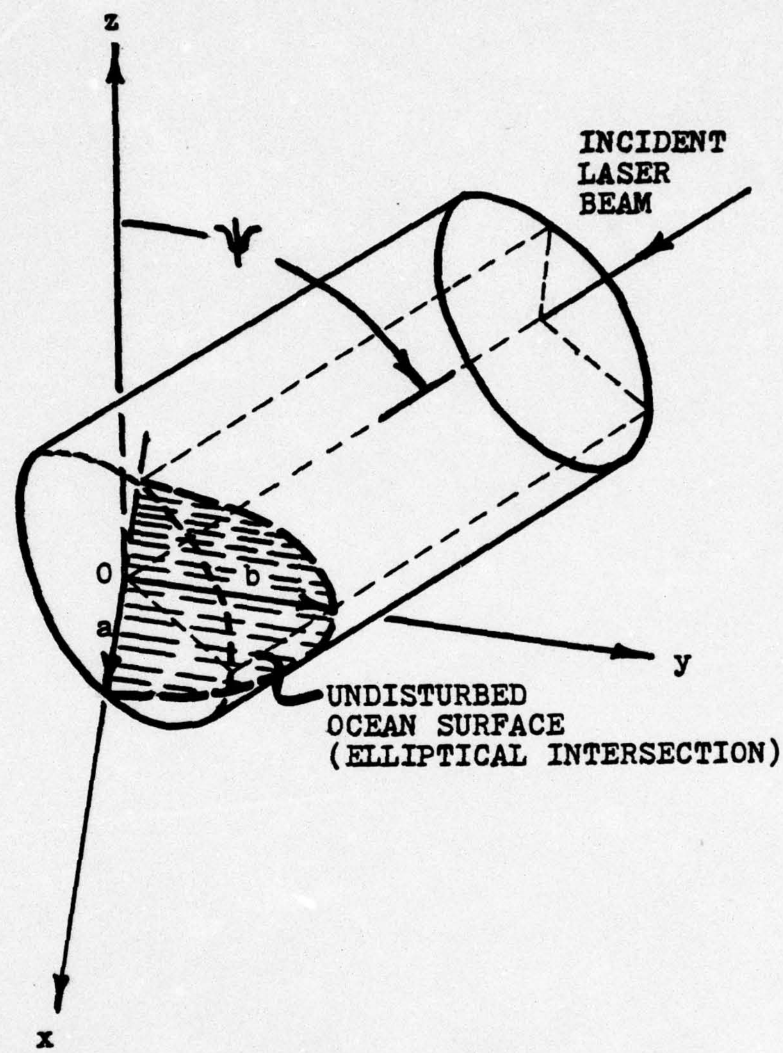

Figure 2: Intersection of laser beam with ocean wave facet

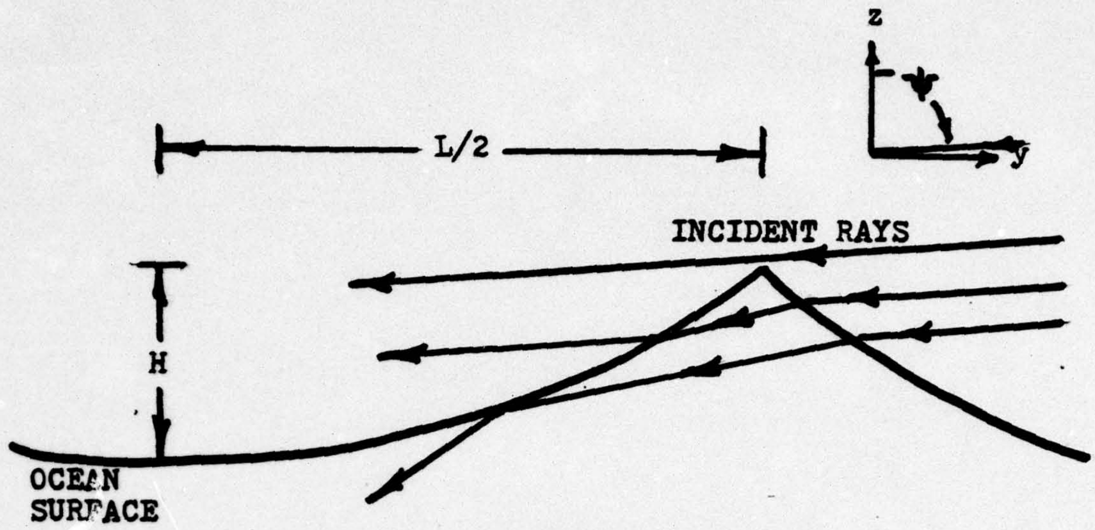

Figure 3: Possible beam paths at high incidence angles

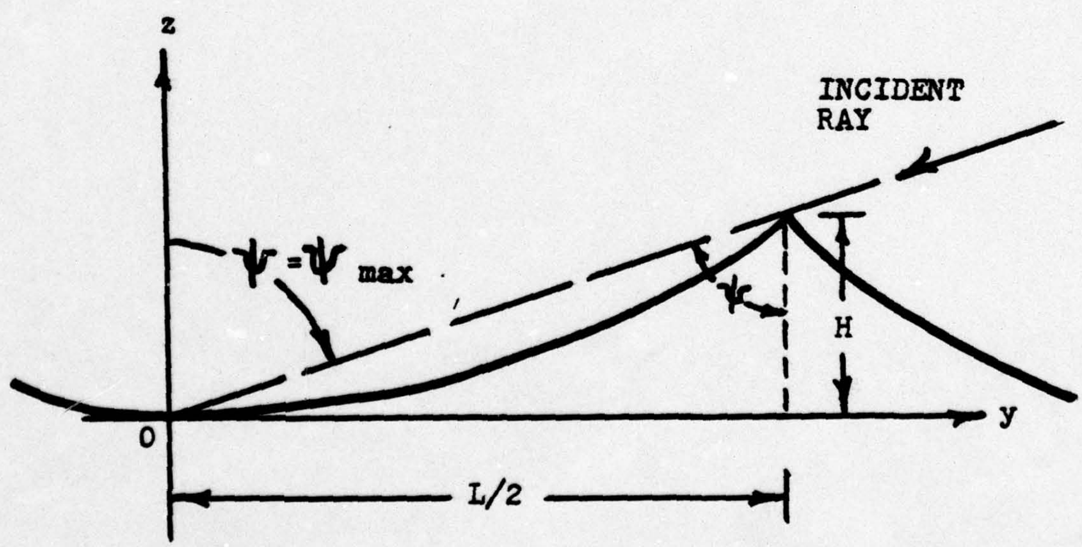

Figure 4: Maximum angle of incidence wave geometry

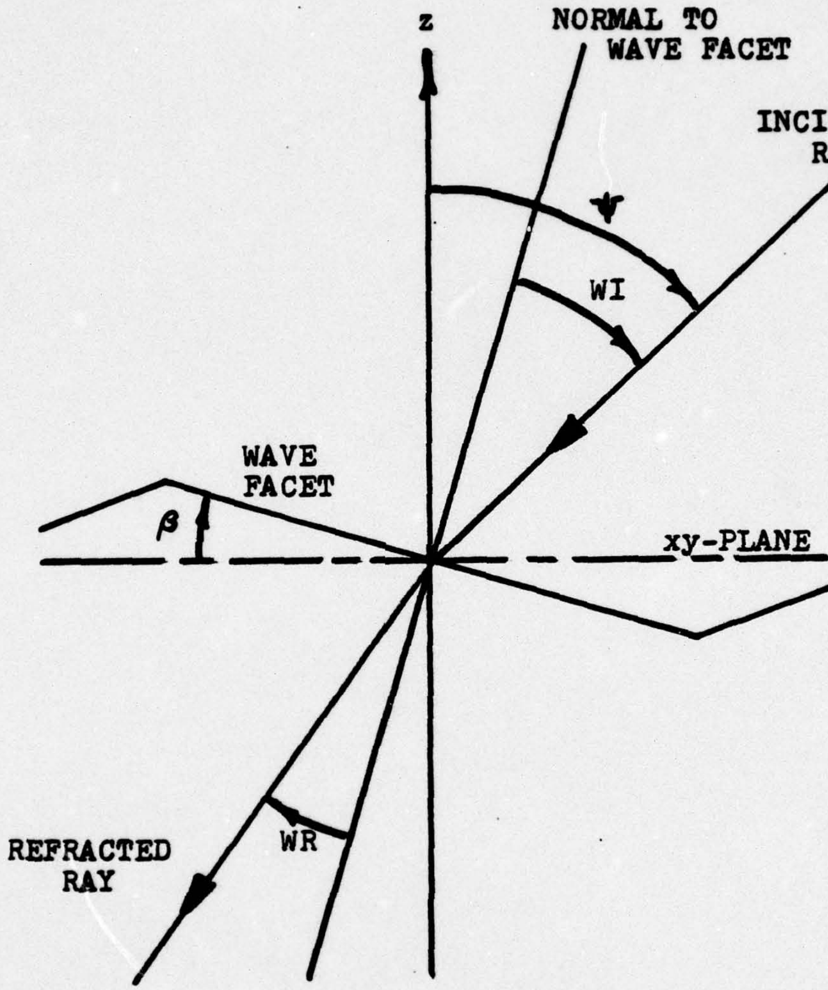

Figure 5: Ray refraction geometry

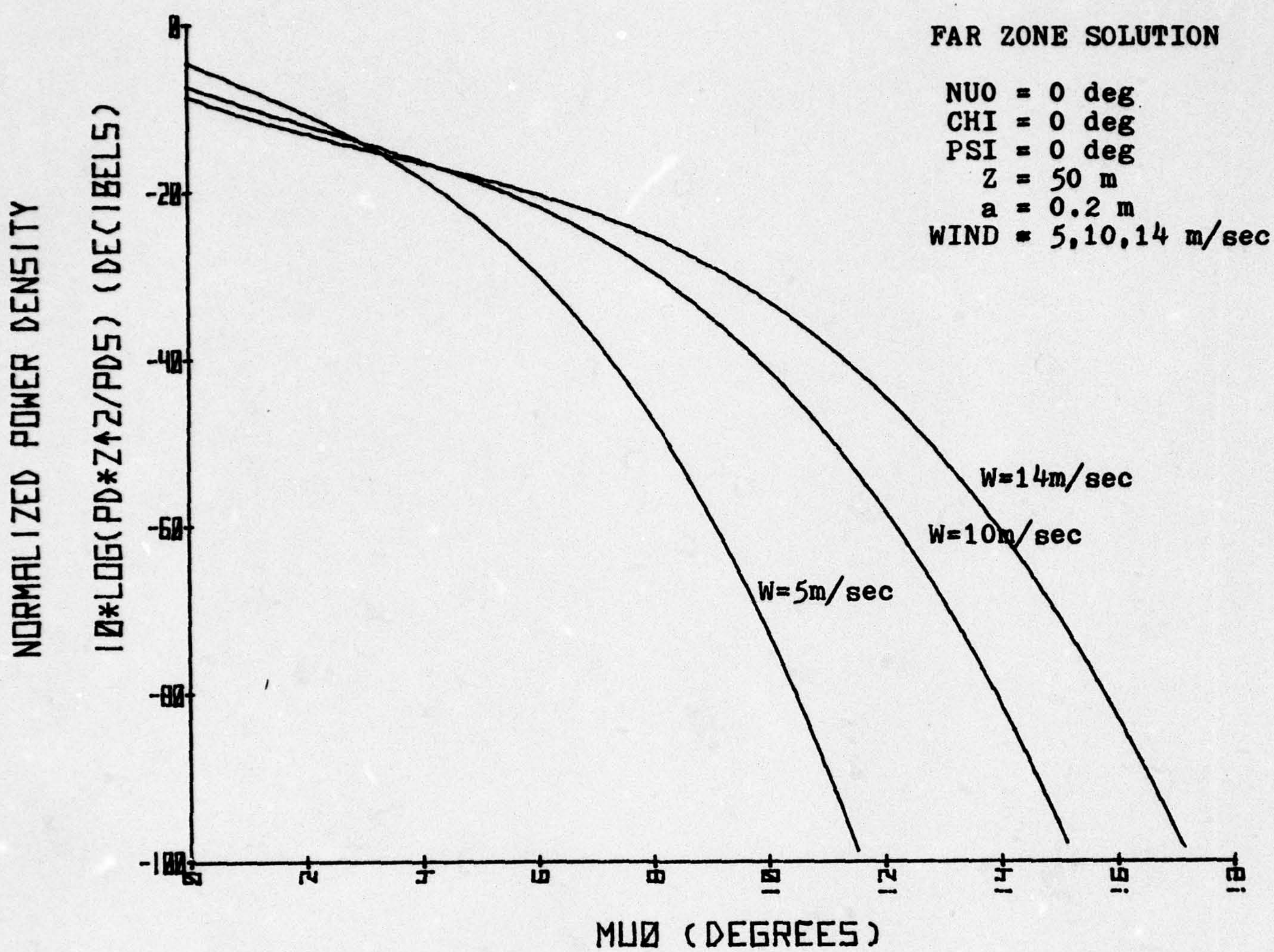
FAR ZONE SOLUTION
NUO = 0 deg
CHI = 0 deg
PSI = 0 deg
Z = 50 m
a = 0.2 m
WIND = 5,10,14 m/sec
W=14m/sec
W=10m/sec
W=5m/sec
NORMALIZED POWER DENSITY
10*LOG(PD*Z↑2/PDS) (DECIBELS)
MU0 (DEGREES)
0
-20
-40
-60
-80
-100
0
2
4
6
8
10
12
14
16
18

Figure 6

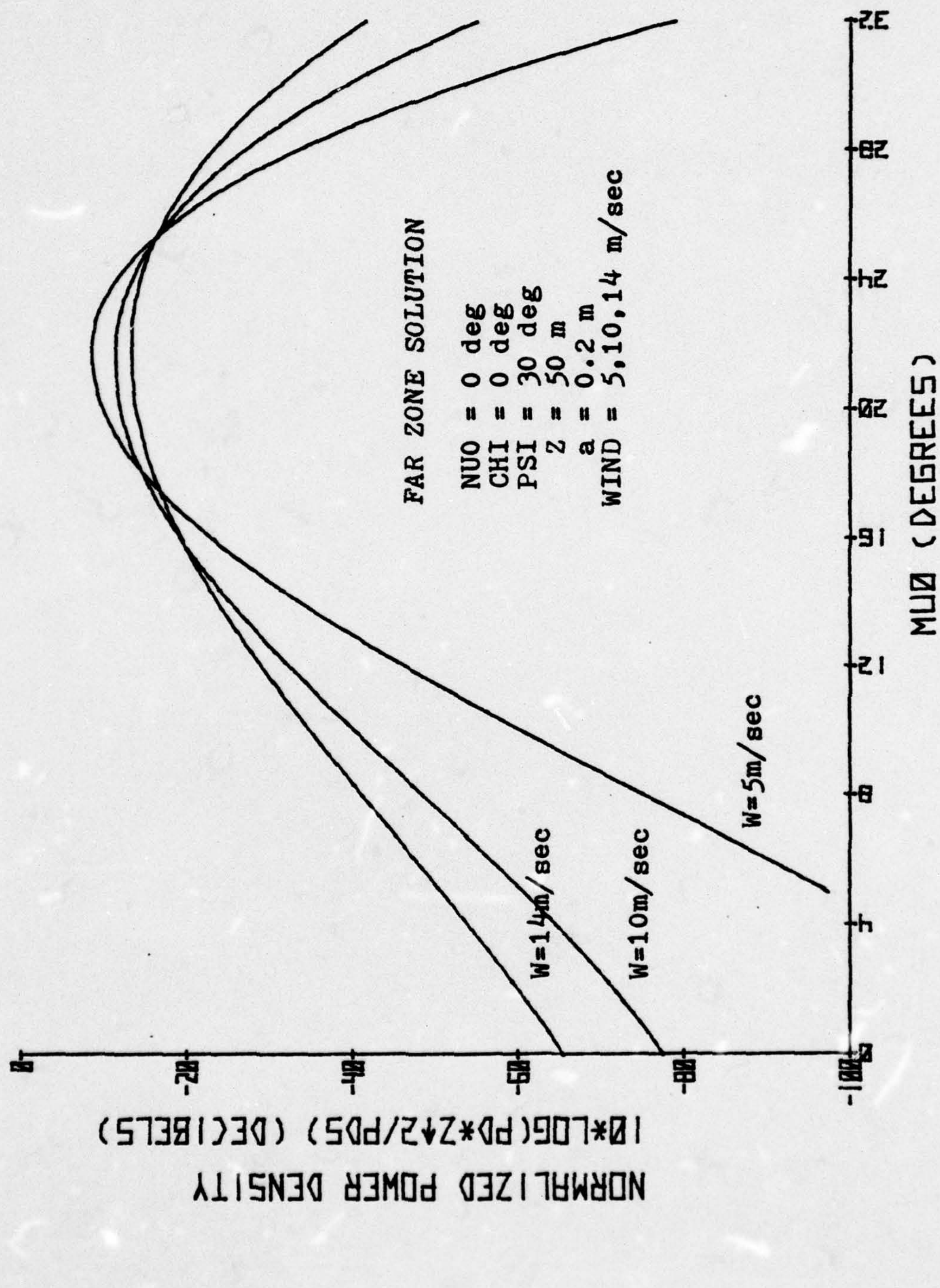
NORMALIZED POWER DENSITY
10*LOG(PD*Z↑2/PDS) (DECIBELS)
0
-20
-40
-60
-80
-100
0
4
8
12
16
20
24
28
32
MUØ (DEGREES)
FAR ZONE SOLUTION
NUO = 0 deg
CHI = 0 deg
PSI = 30 deg
Z = 50 m
a = 0.2 m
WIND = 5,10,14 m/sec
W=14m/sec
W=10m/sec
W=5m/sec

Figure 7

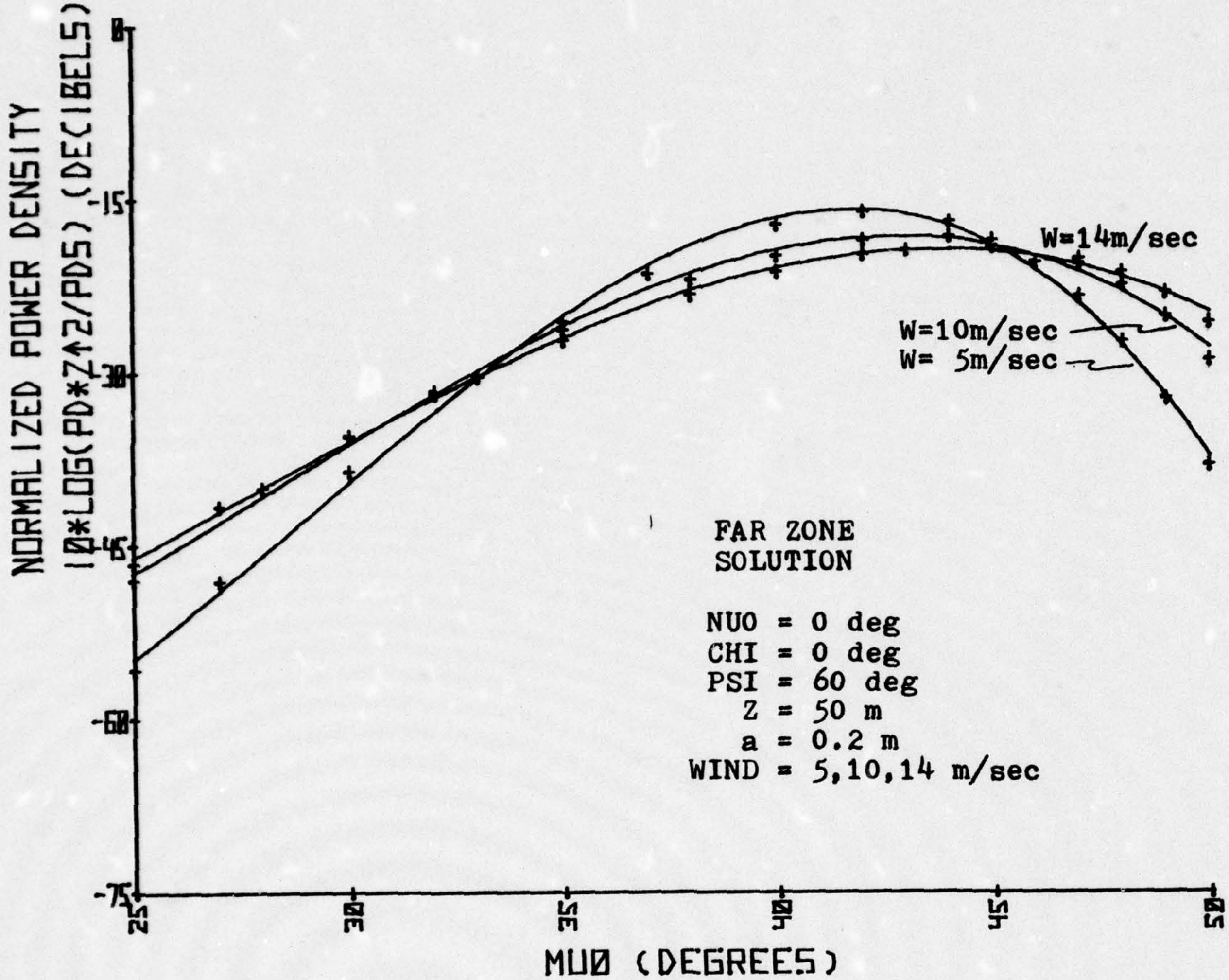
NORMALIZED POWER DENSITY
10*LOG(PD*Z↑2/PDS),(DECIBELS)
0
-15
-30
-45
-60
-75
25
30
35
40
45
50
MUØ (DEGREES)
W=14m/sec
W=10m/sec
W= 5m/sec
FAR ZONE
SOLUTION
NUO = 0 deg
CHI = 0 deg
PSI = 60 deg
Z = 50 m
a = 0.2 m
WIND = 5,10,14 m/sec

Figure 8

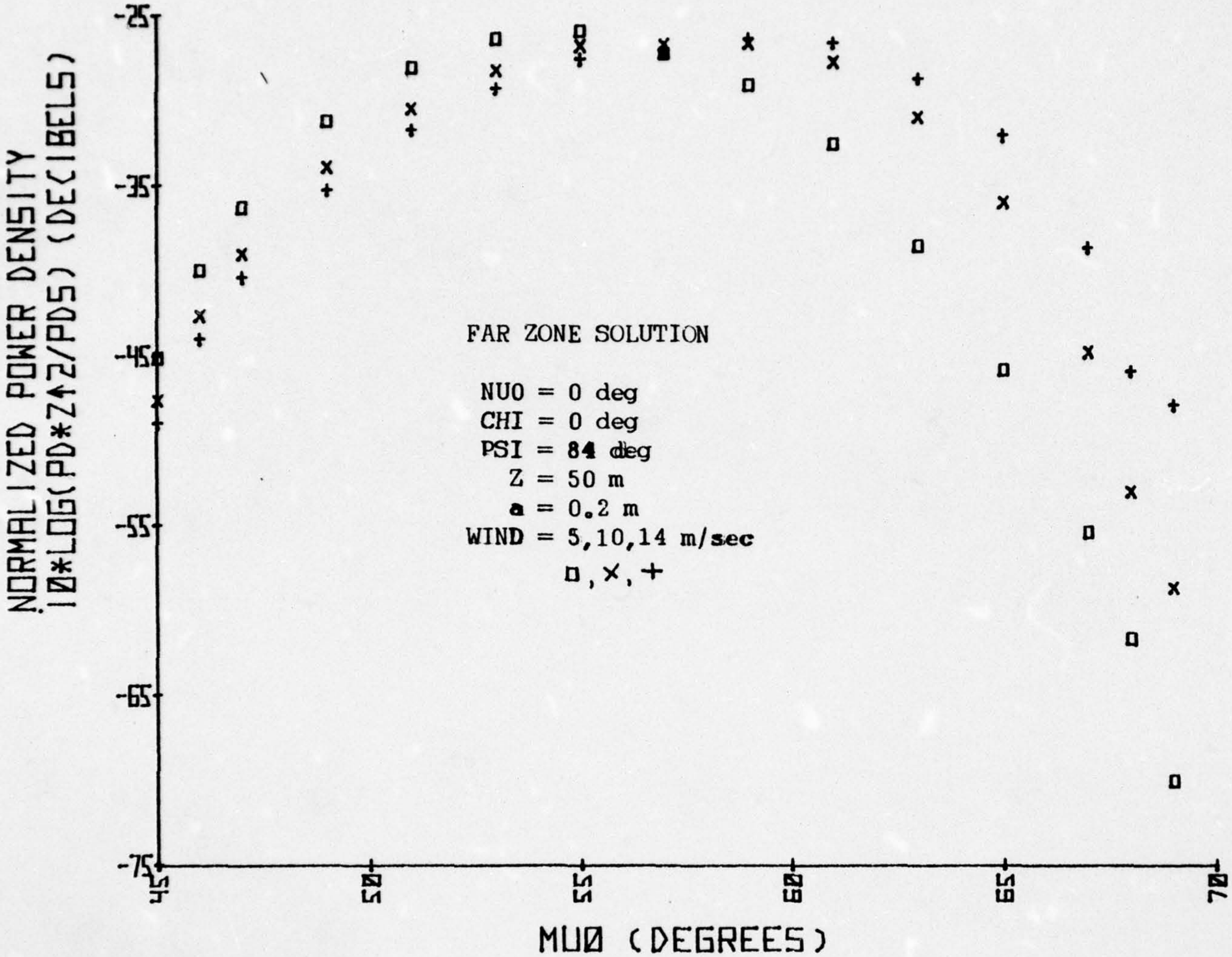
NORMALIZED POWER DENSITY
10*LOG(PD*Z↑2/PDS) (DECIBELS)
-25
-35
-45
-55
-65
-75
45
50
55
60
65
70
MUØ (DEGREES)
FAR ZONE SOLUTION
NUO = 0 deg
CHI = 0 deg
PSI = 84 deg
Z = 50 m
a = 0.2 m
WIND = 5,10,14 m/sec
□, ×, +

Figure 9

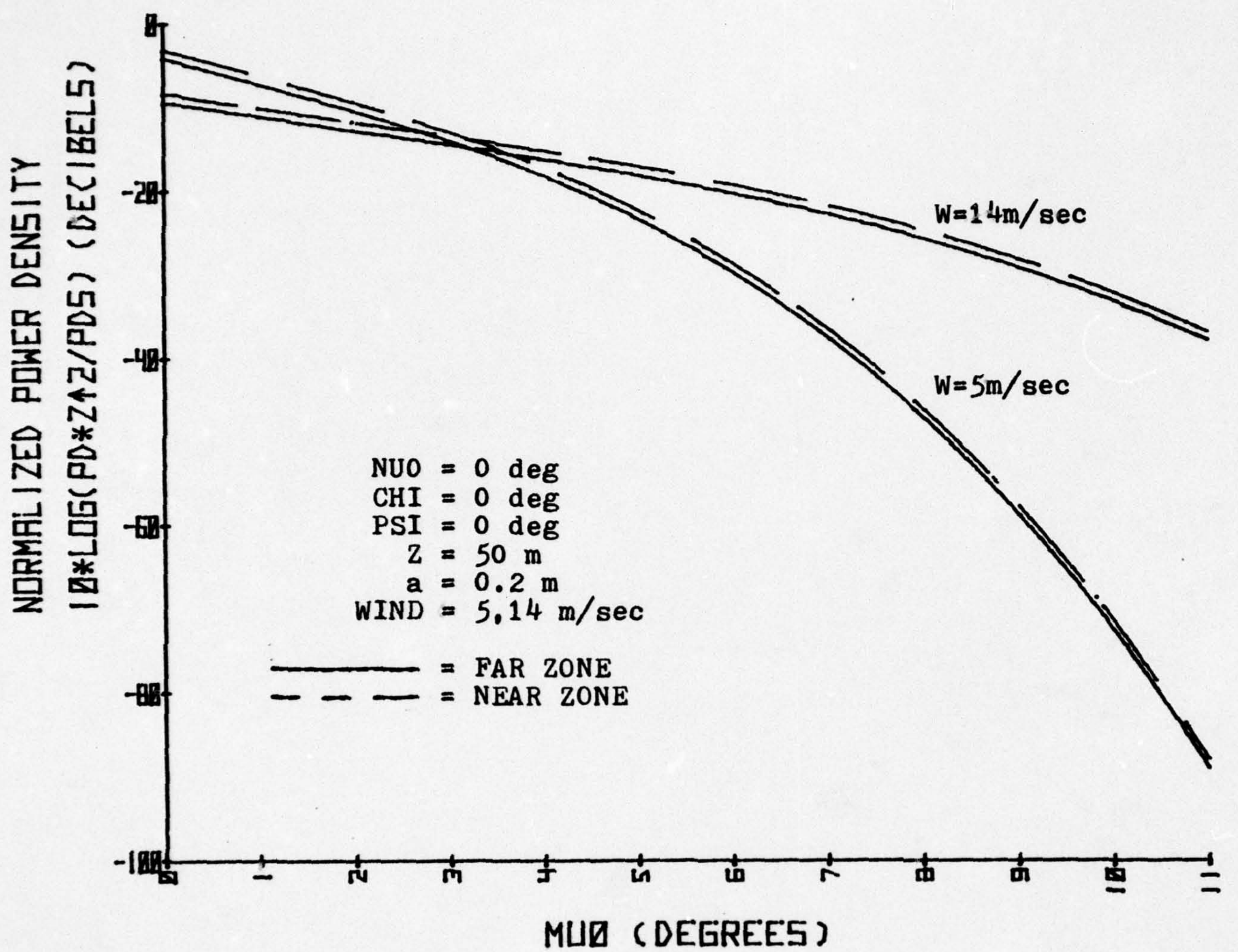

NORMALIZED POWER DENSITY
10*LOG(PD*Z↑2/PDS) (DECIBELS)
0
-20
-40
-60
-80
-100
0
1
2
3
4
5
6
7
8
9
10
11
MU0 (DEGREES)
W=14m/sec
W=5m/sec
NUO = 0 deg
CHI = 0 deg
PSI = 0 deg
Z = 50 m
a = 0.2 m
WIND = 5,14 m/sec
= FAR ZONE
= NEAR ZONE

Figure 10

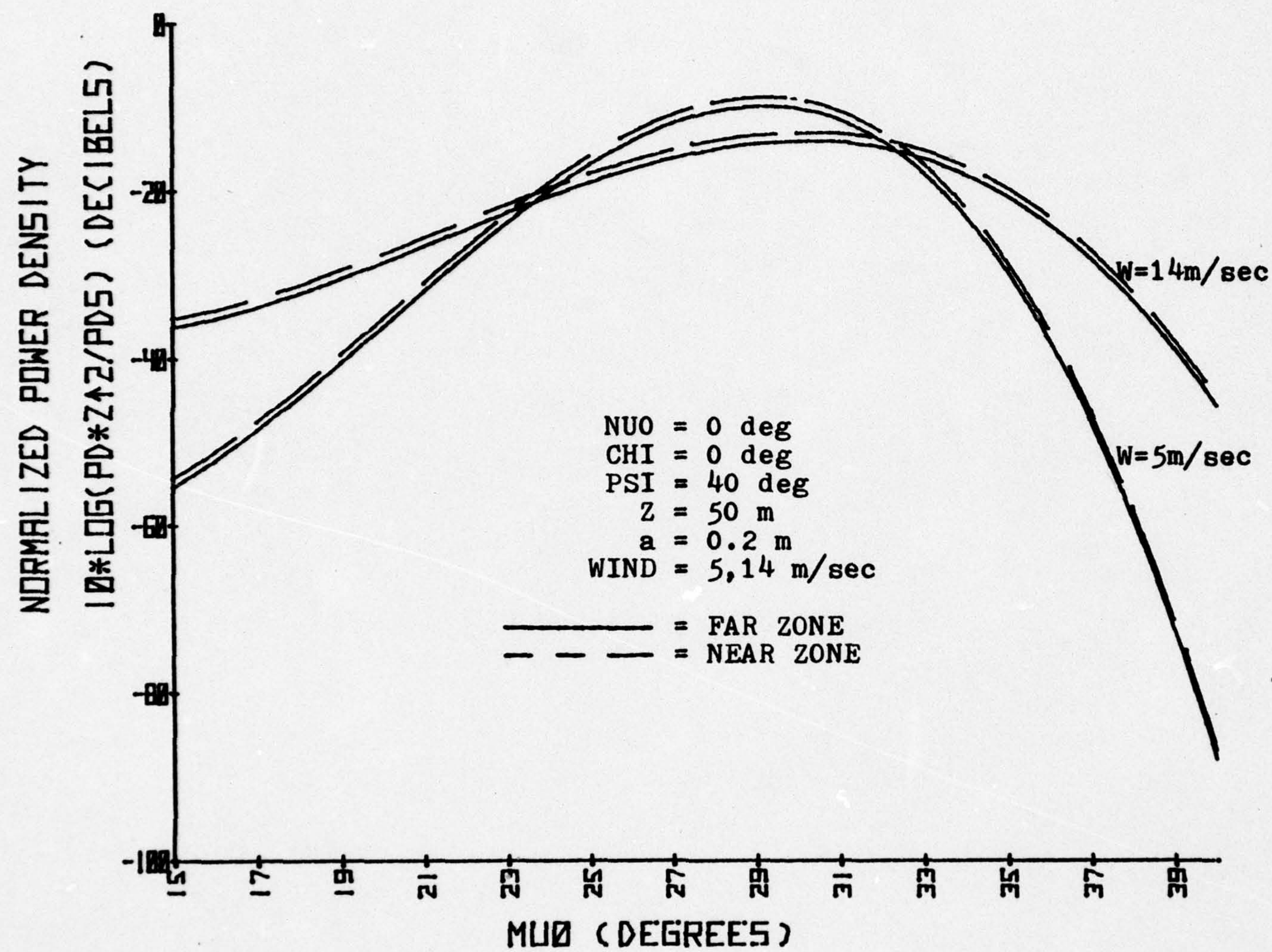
NORMALIZED POWER DENSITY
10*LOG(PD*Z↑2/PDS) (DECIBELS)
0
-20
-40
-60
-80
-100
15
17
19
21
23
25
27
29
31
33
35
37
39
MUØ (DEGREES)
W=14m/sec
W=5m/sec
NUO = 0 deg
CHI = 0 deg
PSI = 40 deg
Z = 50 m
a = 0.2 m
WIND = 5,14 m/sec
= FAR ZONE
= NEAR ZONE

Figure 11

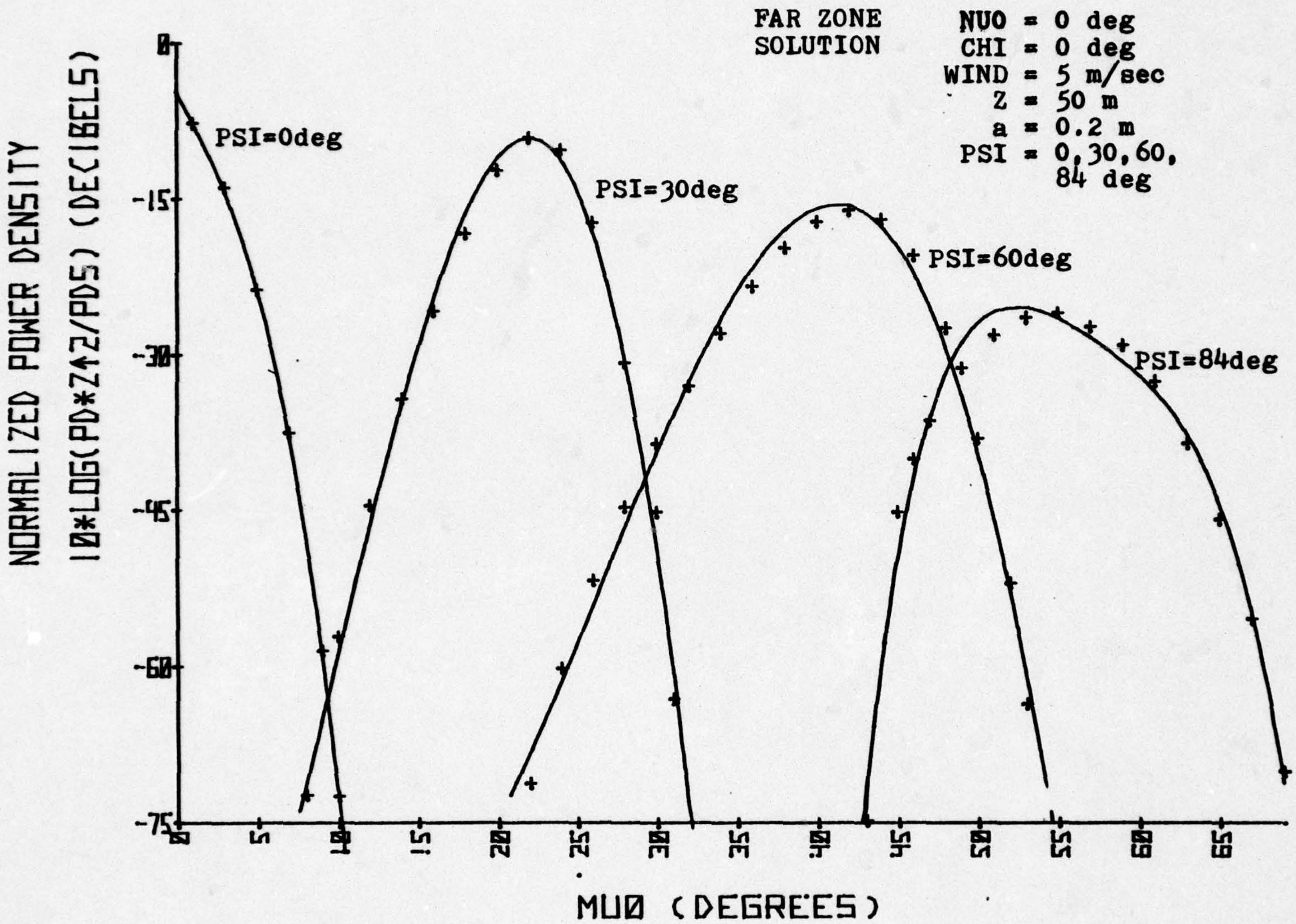
FAR ZONE
SOLUTION
NUO = 0 deg
CHI = 0 deg
WIND = 5 m/sec
Z = 50 m
a = 0.2 m
PSI = 0,30,60,
84 deg
PSI=0deg
PSI=30deg
PSI=60deg
PSI=84deg
NORMALIZED POWER DENSITY
10*LOG(PD*Z↑2/PDS) (DECIBELS)
0
-15
-30
-45
-60
-75
0
5
10
15
20
25
30
35
40
45
50
55
60
65
MU0 (DEGREES)

Figure 12

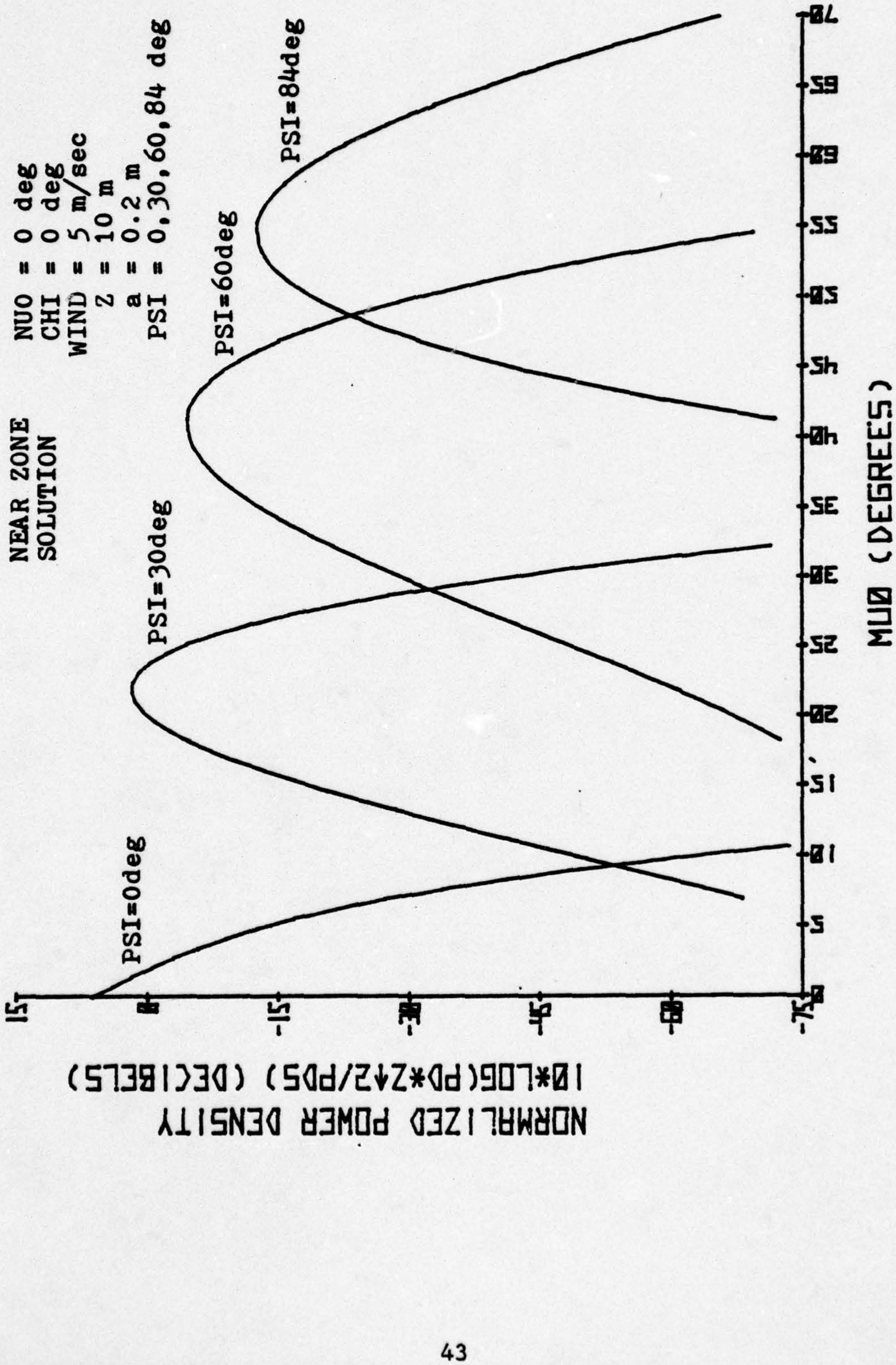
NEAR ZONE
SOLUTION
NUO = 0 deg
CHI = 0 deg
WIND = 5 m/sec
Z = 10 m
a = 0.2 m
PSI = 0,30,60,84 deg
PSI=0deg
PSI=30deg
PSI=60deg
PSI=84deg
NORMALIZED POWER DENSITY
10*LOG(PD*Z↑2/PDS) (DECIBELS)
MUØ (DEGREES)
15
-15
-45
-75
0
5
10
15
20
25
30
35
40
45
50
55
60
65
70

Figure 13

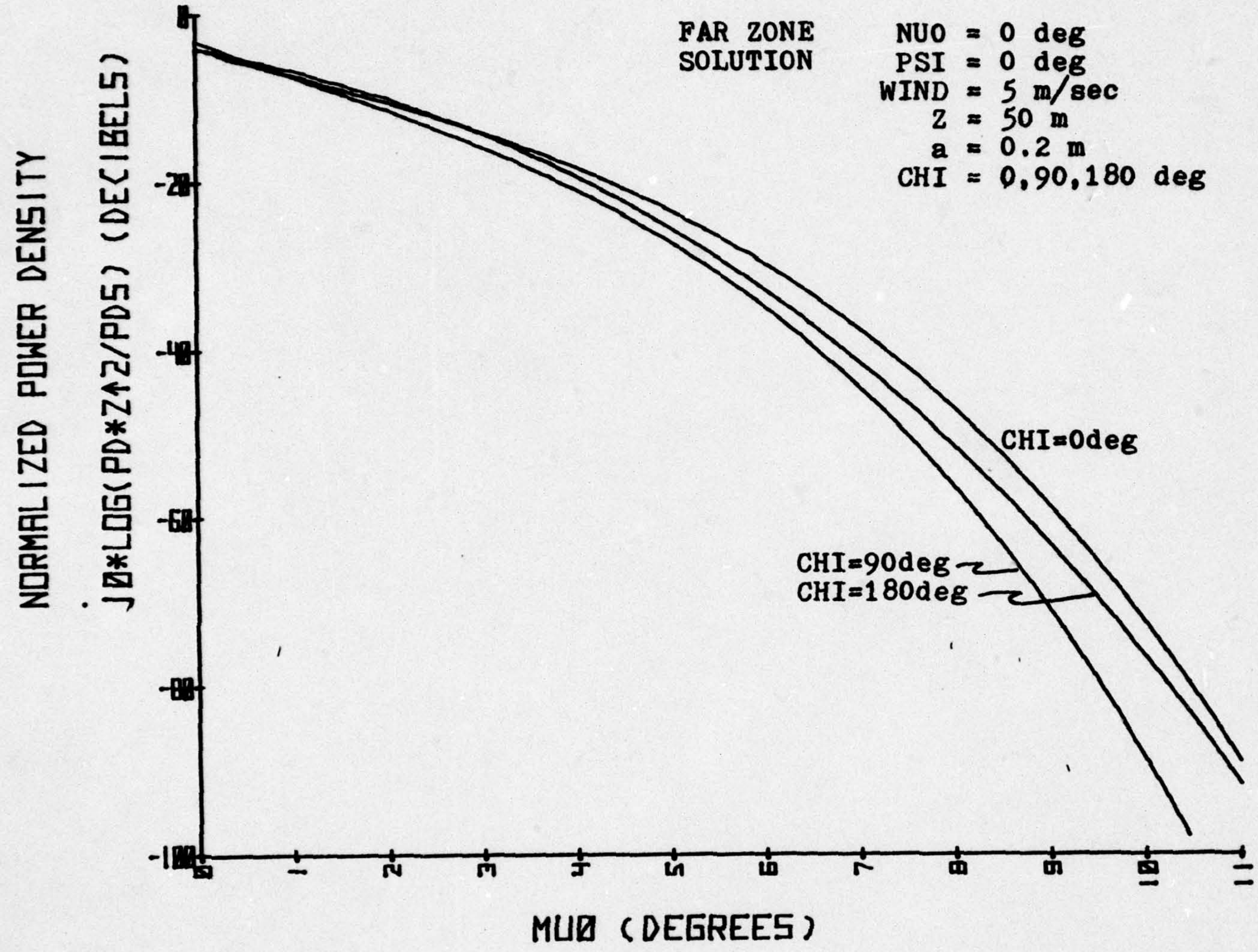
NORMALIZED POWER DENSITY
1Ø*LOG(PD*Z↑2/PDS) (DECIBELS)
MUØ (DEGREES)
FAR ZONE
SOLUTION
NUO = 0 deg
PSI = 0 deg
WIND = 5 m/sec
Z = 50 m
a = 0.2 m
CHI = 0,90,180 deg
CHI=0deg
CHI=90deg
CHI=180deg
0
-20
-40
-60
-80
-100
0
1
2
3
4
5
6
7
8
9
10
11

Figure 14

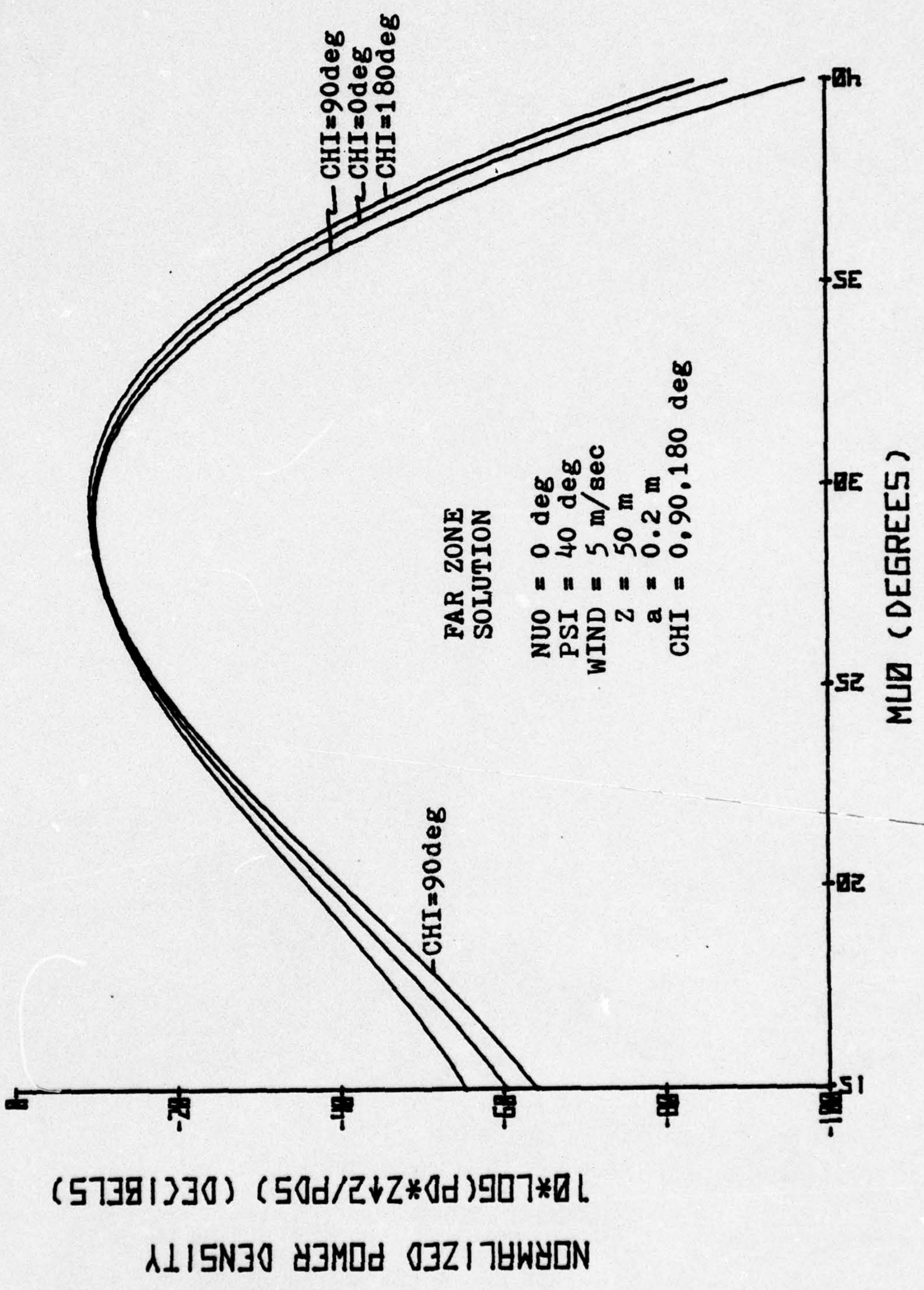
CHI=90deg
CHI=0deg
CHI=180deg
CHI=90deg
FAR ZONE
SOLUTION
NUO = 0 deg
PSI = 40 deg
WIND = 5 m/sec
Z = 50 m
a = 0.2 m
CHI = 0,90,180 deg
15
20
25
30
35
40
MUØ (DEGREES)
0
-20
-40
-60
-80
-100
NORMALIZED POWER DENSITY
10*LOG(PD*Z↑2/PDS) (DECIBELS)

Figure 15

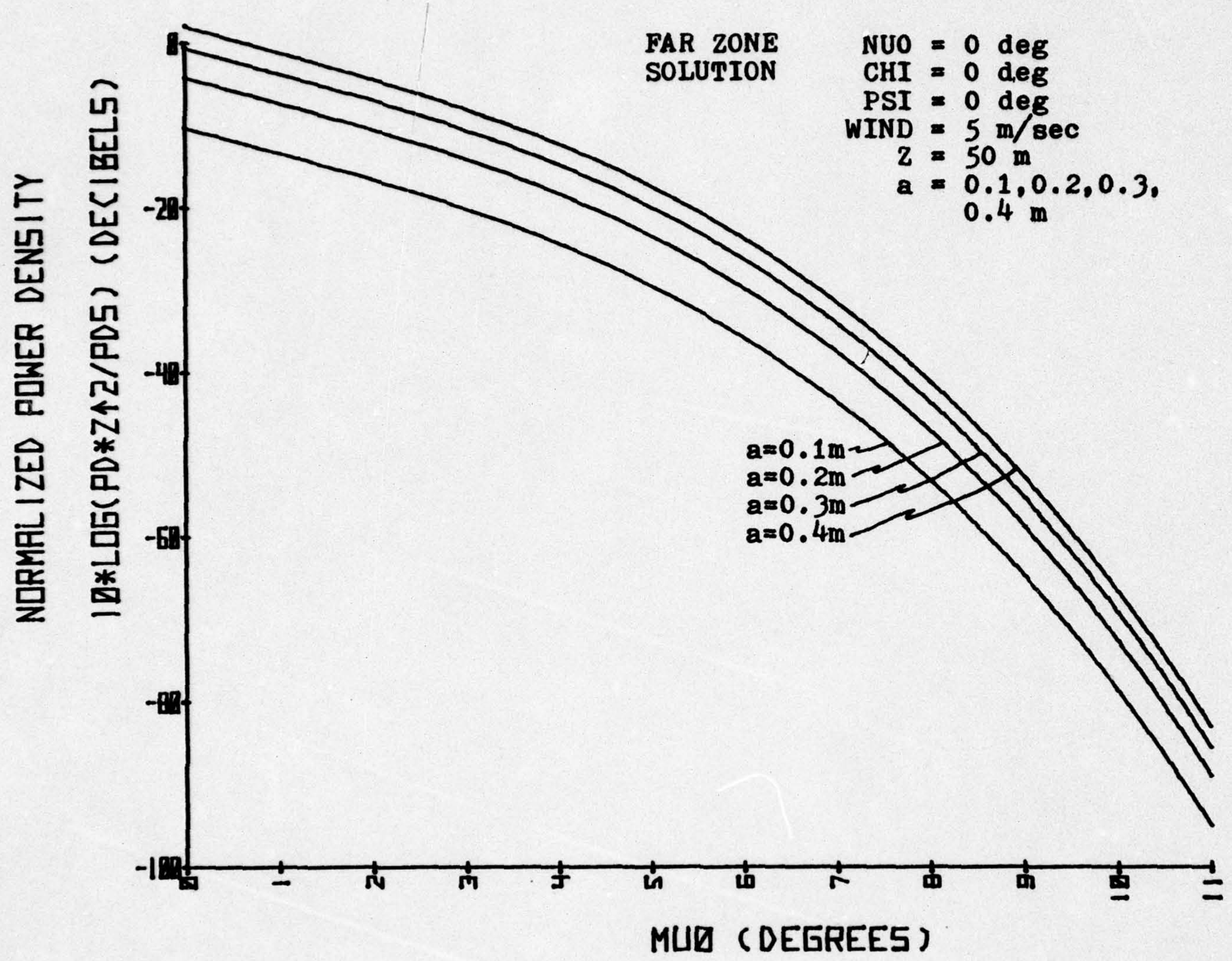
FAR ZONE
SOLUTION
NUO = 0 deg
CHI = 0 deg
PSI = 0 deg
WIND = 5 m/sec
Z = 50 m
a = 0.1,0.2,0.3,
0.4 m
a=0.1m
a=0.2m
a=0.3m
a=0.4m
NORMALIZED POWER DENSITY
10*LOG(PD*Z↑2/PDS) (DECIBELS)
0
-20
-40
-60
-80
-100
0
1
2
3
4
5
6
7
8
9
10
11
MUØ (DEGREES)

Figure 16

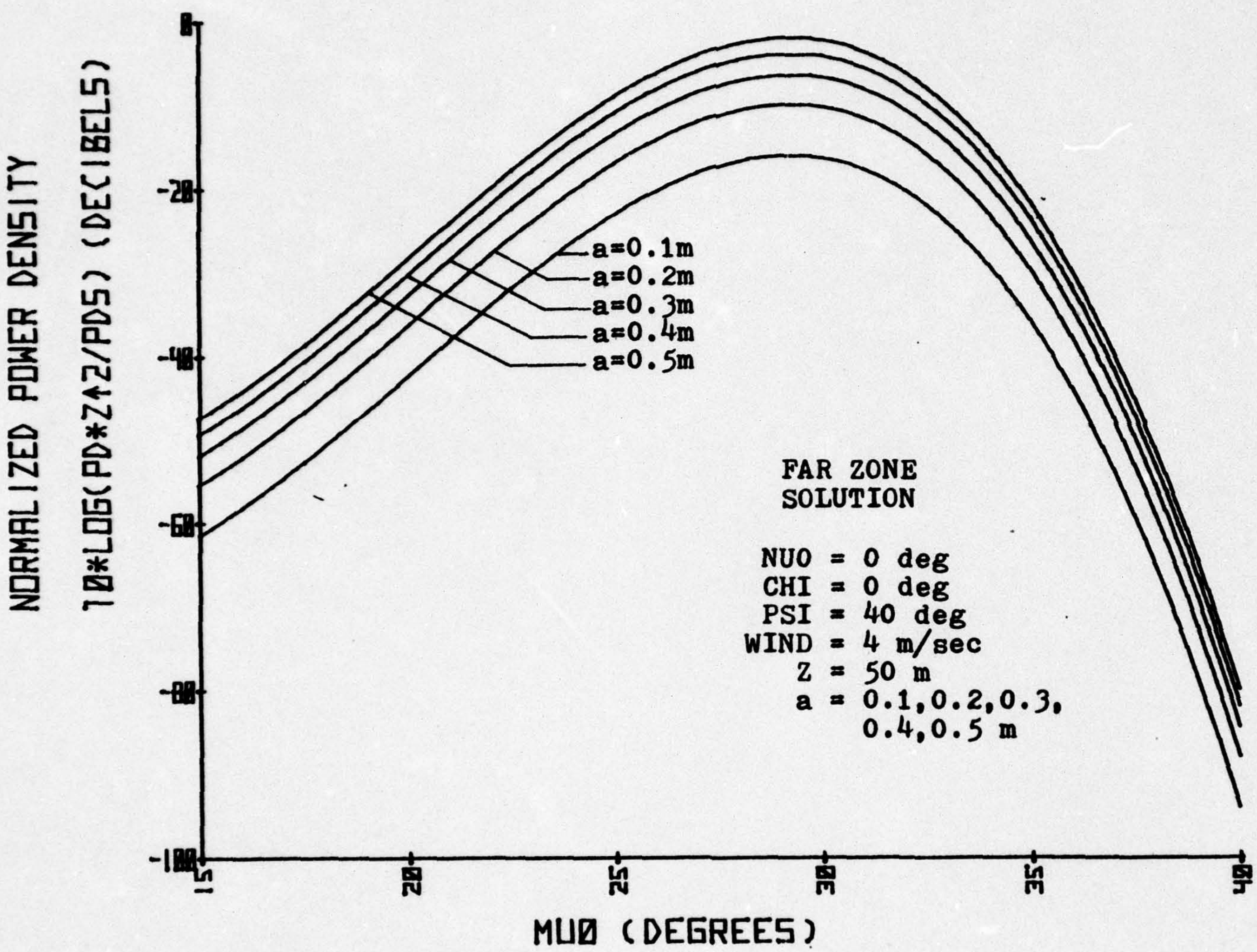
NORMALIZED POWER DENSITY
10*LOG(PD*Z↑2/PDS) (DECIBELS)
0
-20
-40
-60
-80
-100
15
20
25
30
35
40
MUØ (DEGREES)
a=0.1m
a=0.2m
a=0.3m
a=0.4m
a=0.5m
FAR ZONE
SOLUTION
NUO = 0 deg
CHI = 0 deg
PSI = 40 deg
WIND = 4 m/sec
Z = 50 m
a = 0.1,0.2,0.3,
0.4,0.5 m

Figure 17

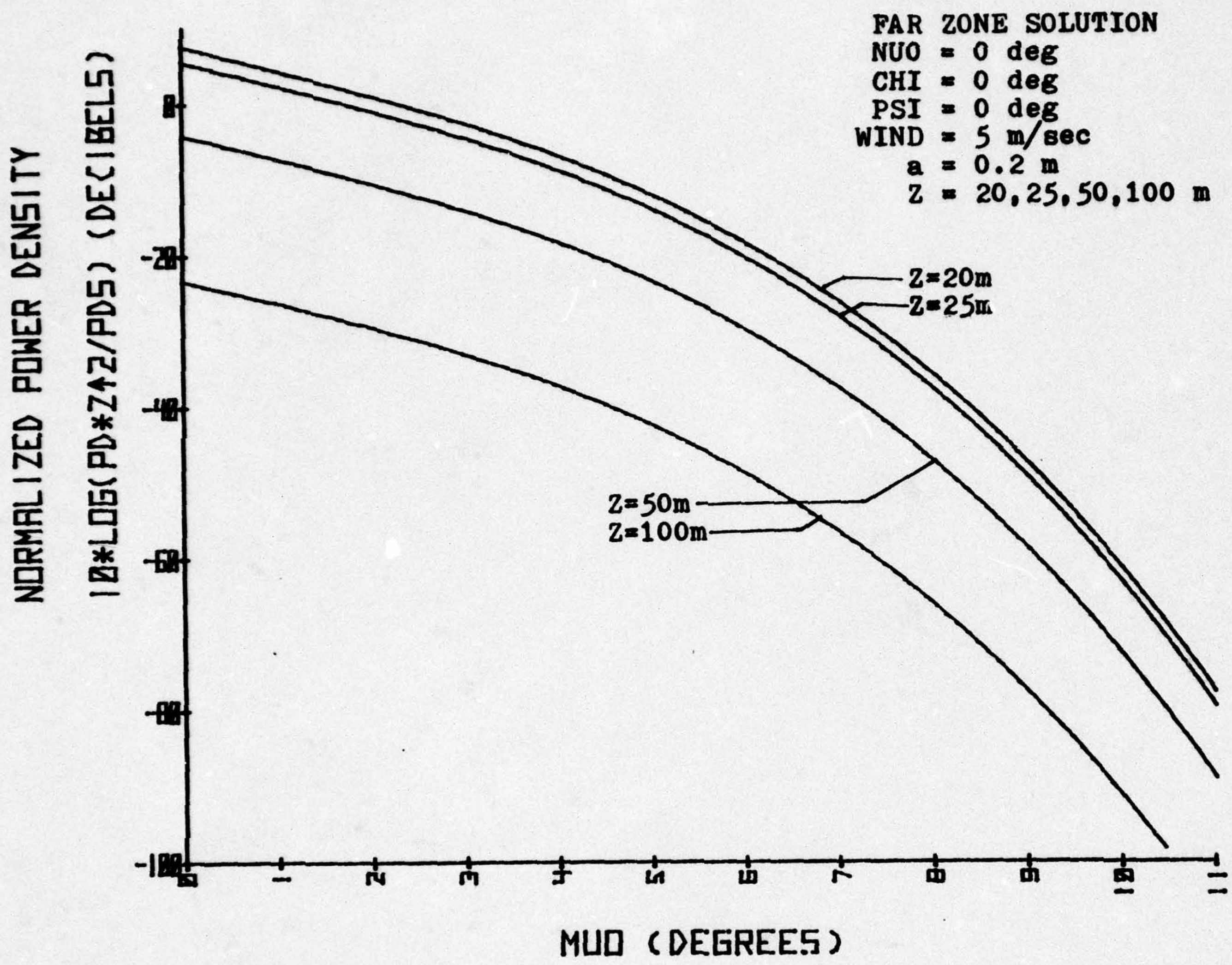
FAR ZONE SOLUTION
NUO = 0 deg
CHI = 0 deg
PSI = 0 deg
WIND = 5 m/sec
a = 0.2 m
Z = 20,25,50,100 m
Z=20m
Z=25m
Z=50m
Z=100m
NORMALIZED POWER DENSITY
10*LOG(PD*Z↑2/PDS) (DECIBELS)
0
-20
-40
-60
-80
-100
0
1
2
3
4
5
6
7
8
9
10
11
MUO (DEGREES)

Figure 18

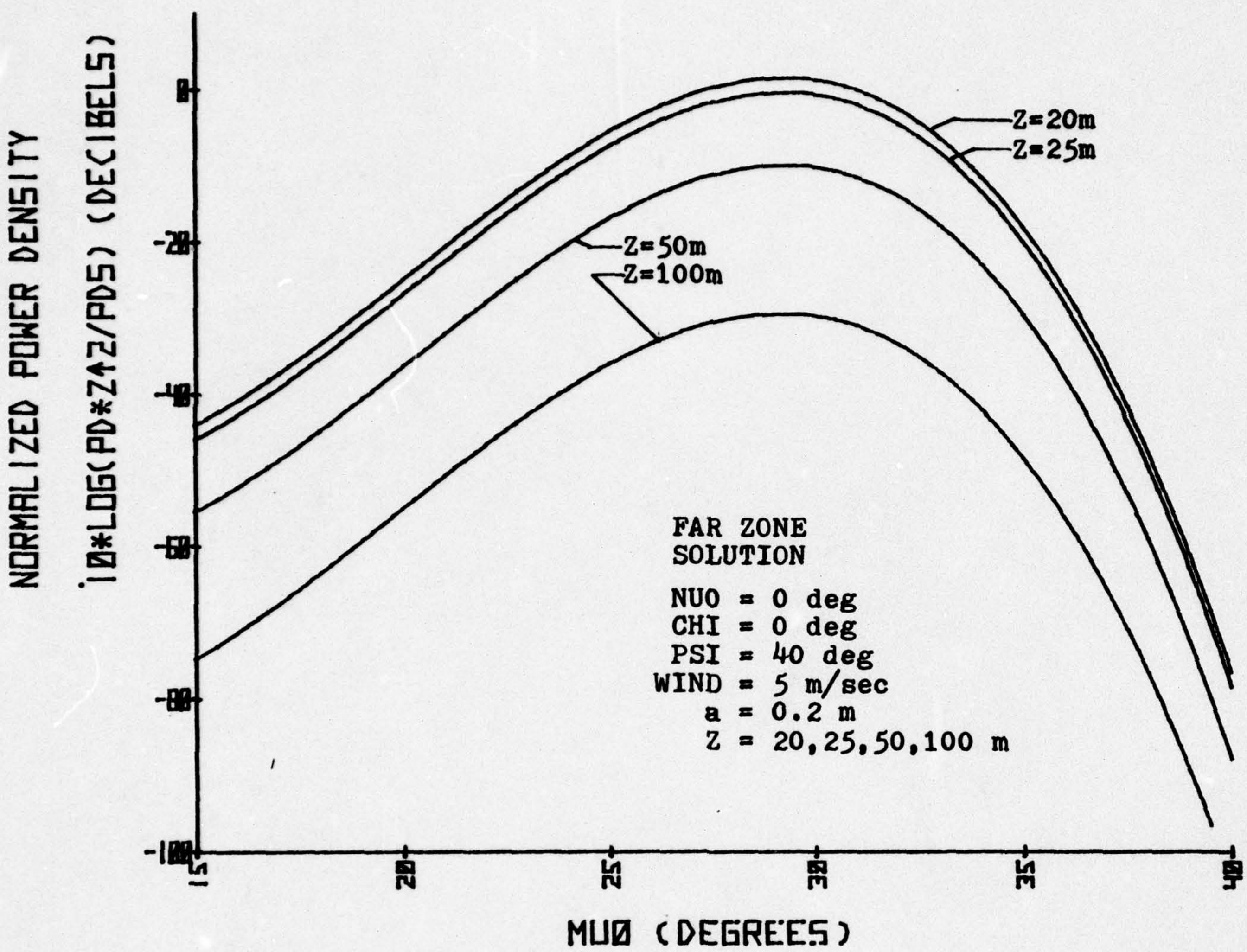
NORMALIZED POWER DENSITY
10*LOG(PD*Z↑2/PDS) (DECIBELS)
0
-20
-40
-60
-80
-100
15
20
25
30
35
40
MUØ (DEGREES)
Z=20m
Z=25m
Z=50m
Z=100m
FAR ZONE
SOLUTION
NUO = 0 deg
CHI = 0 deg
PSI = 40 deg
WIND = 5 m/sec
a = 0.2 m
Z = 20,25,50,100 m

Figure 19

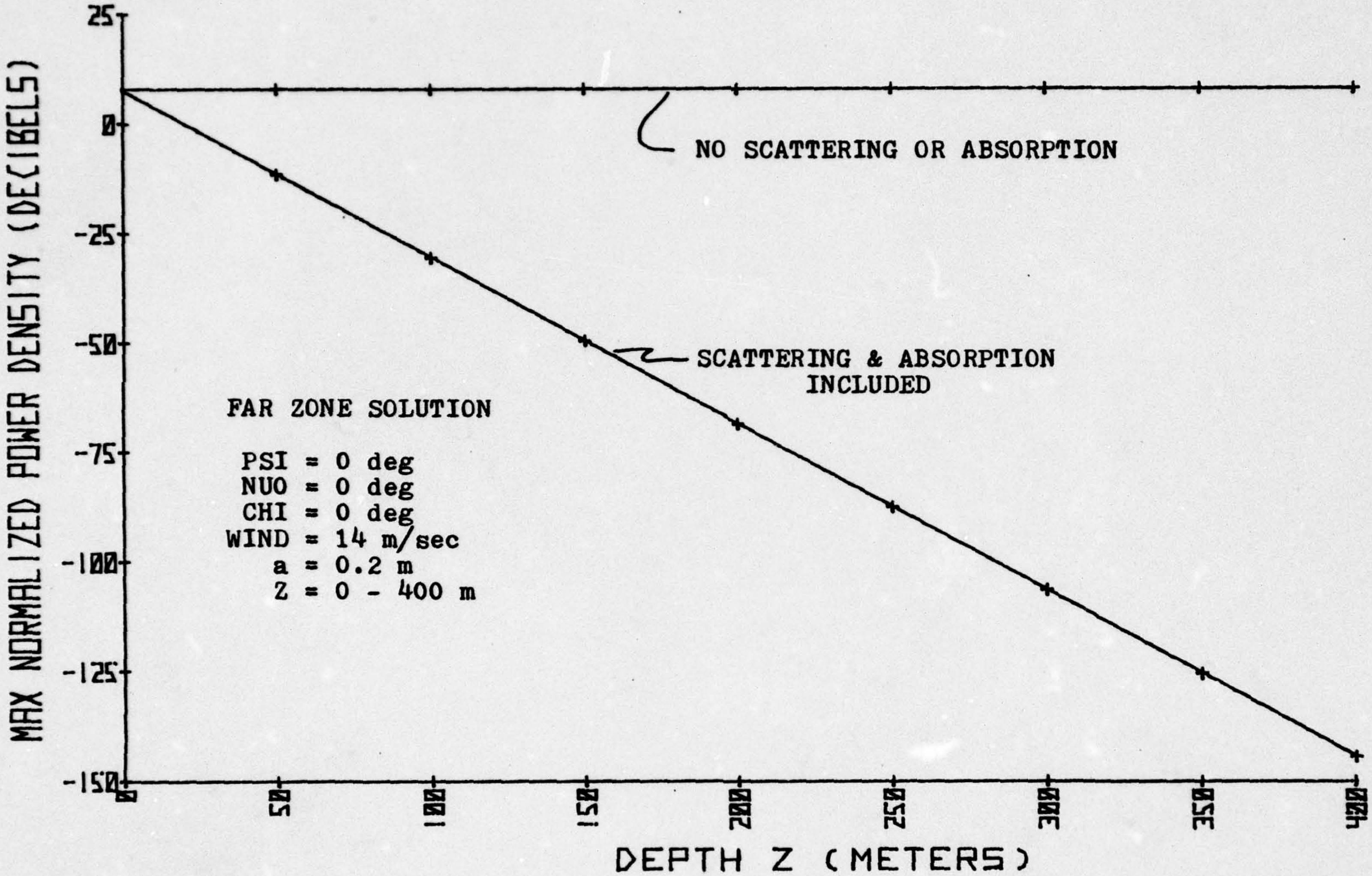
25
0
-25
-50
-75
-100
-125
-150
MAX NORMALIZED POWER DENSITY (DECIBELS)
0
50
100
150
200
250
300
350
400
DEPTH Z (METERS)
NO SCATTERING OR ABSORPTION
SCATTERING & ABSORPTION INCLUDED
FAR ZONE SOLUTION
PSI = 0 deg
NUO = 0 deg
CHI = 0 deg
WIND = 14 m/sec
a = 0.2 m
Z = 0 - 400 m

Figure 20

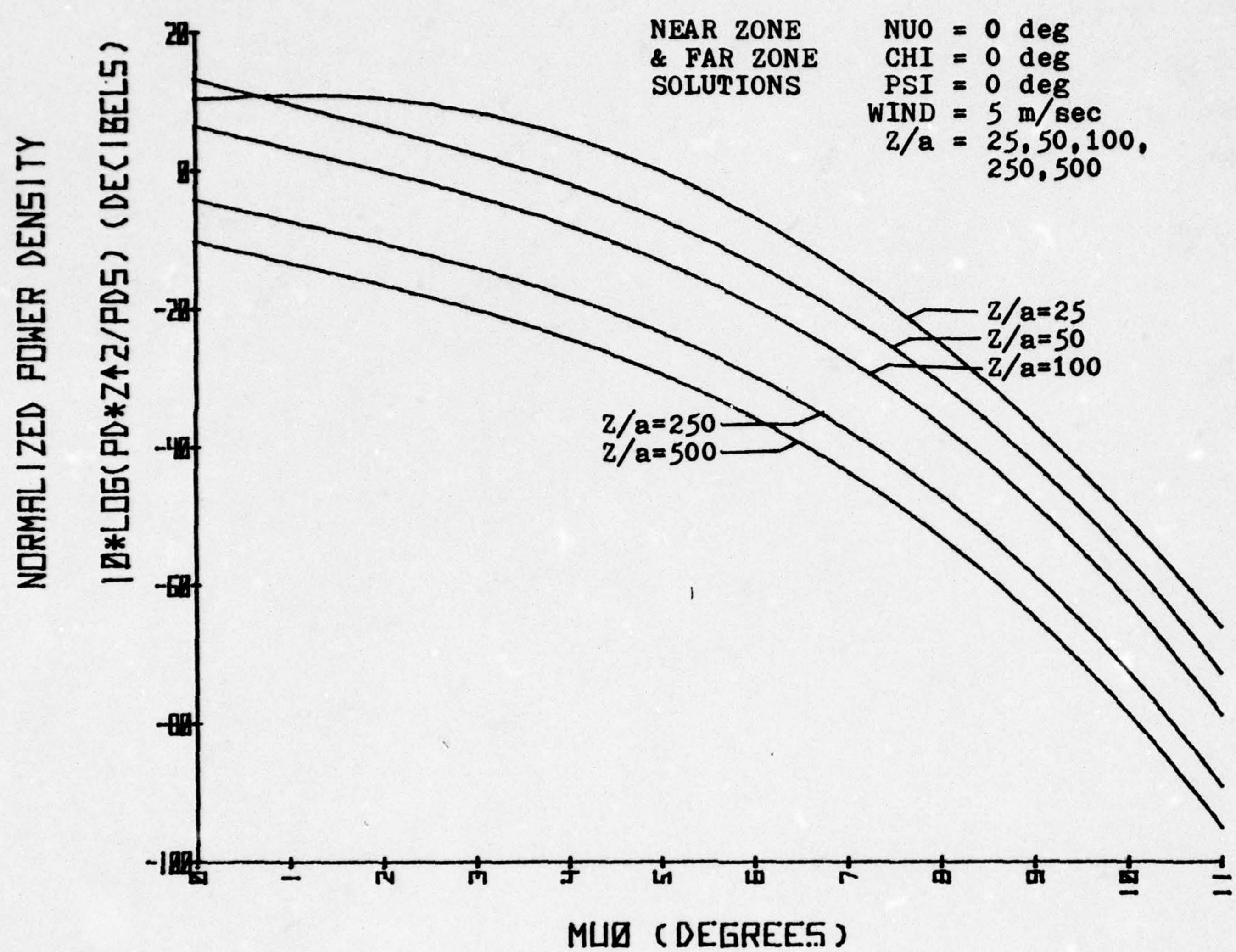
NEAR ZONE
& FAR ZONE
SOLUTIONS
NUO = 0 deg
CHI = 0 deg
PSI = 0 deg
WIND = 5 m/sec
Z/a = 25,50,100,
250,500
Z/a=25
Z/a=50
Z/a=100
Z/a=250
Z/a=500
NORMALIZED POWER DENSITY
10*LOG(PD*Z↑2/PDS) (DECIBELS)
20
0
-20
-40
-60
-80
-100
0
1
2
3
4
5
6
7
8
9
10
11
MUØ (DEGREES)

Figure 21

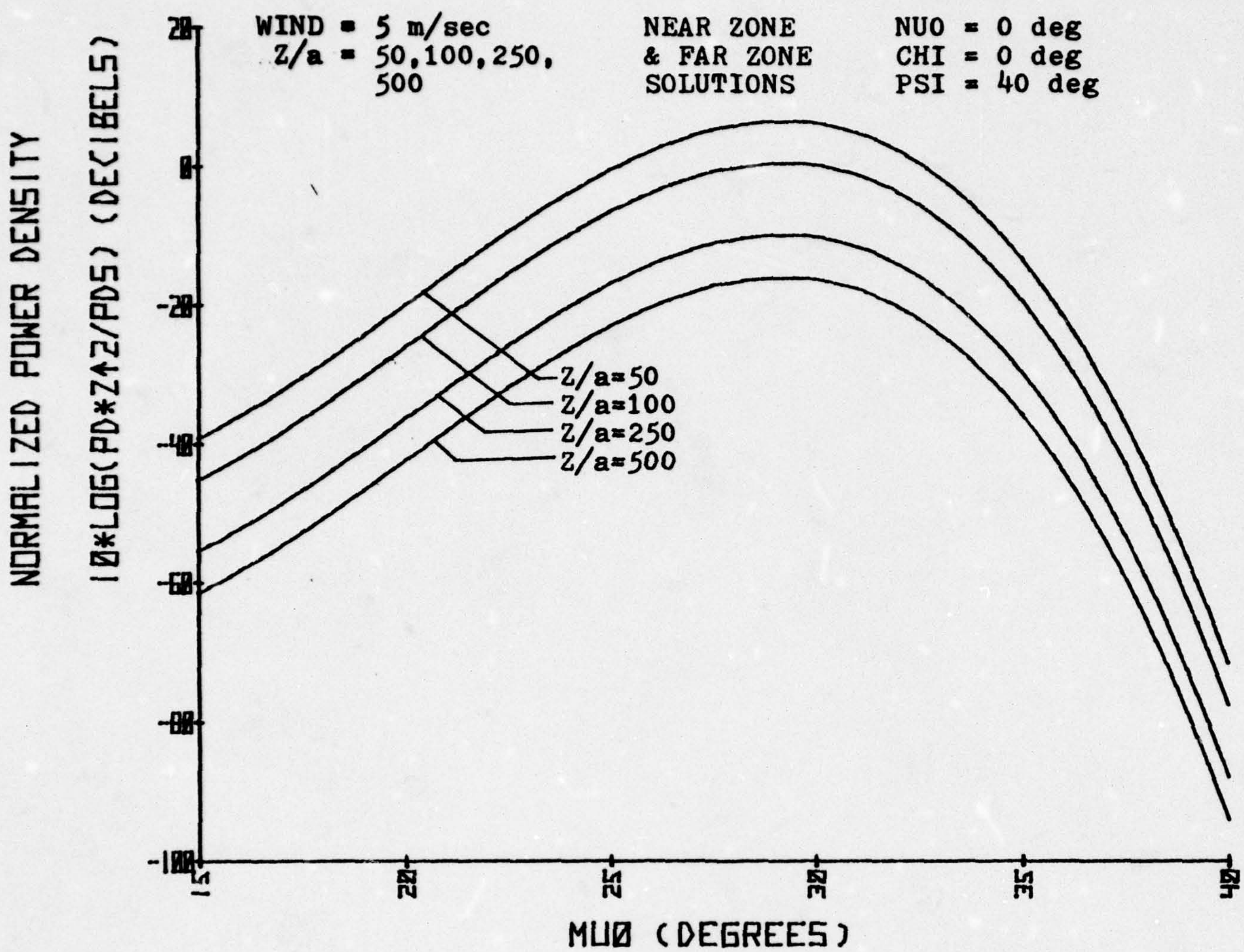
WIND = 5 m/sec
Z/a = 50,100,250,
500
NEAR ZONE
& FAR ZONE
SOLUTIONS
NUO = 0 deg
CHI = 0 deg
PSI = 40 deg
NORMALIZED POWER DENSITY
10*LOG(PD*Z↑2/PDS) (DECIBELS)
20
0
-20
-40
-60
-80
-100
Z/a=50
Z/a=100
Z/a=250
Z/a=500
15
20
25
30
35
40
MU0 (DEGREES)

Figure 22

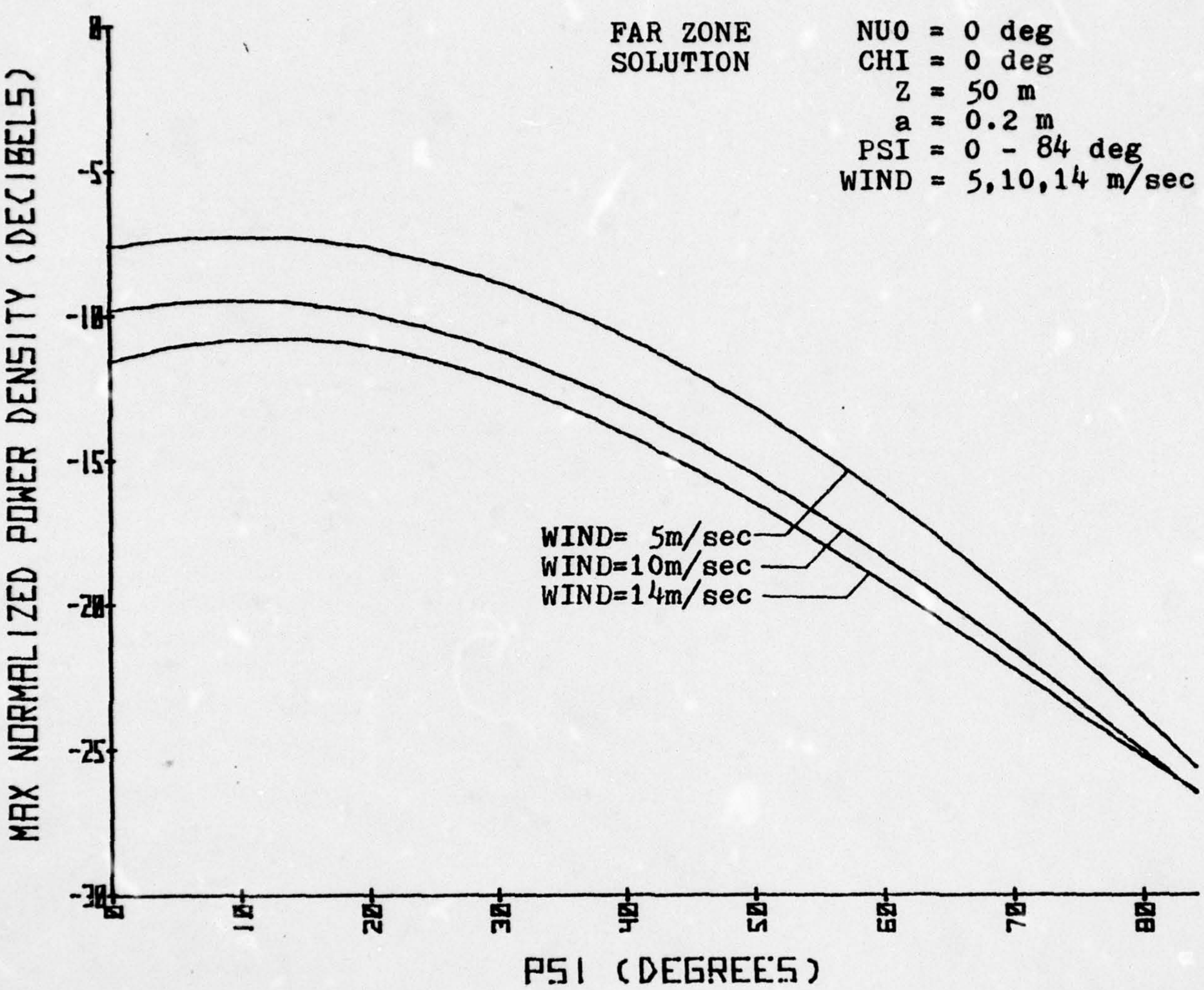
FAR ZONE
SOLUTION
NUO = 0 deg
CHI = 0 deg
Z = 50 m
a = 0.2 m
PSI = 0 - 84 deg
WIND = 5,10,14 m/sec
WIND= 5m/sec
WIND=10m/sec
WIND=14m/sec
MAX NORMALIZED POWER DENSITY (DECIBELS)
PSI (DEGREES)
0
-5
-10
-15
-20
-25
-30
0
10
20
30
40
50
60
70
80

Figure 23

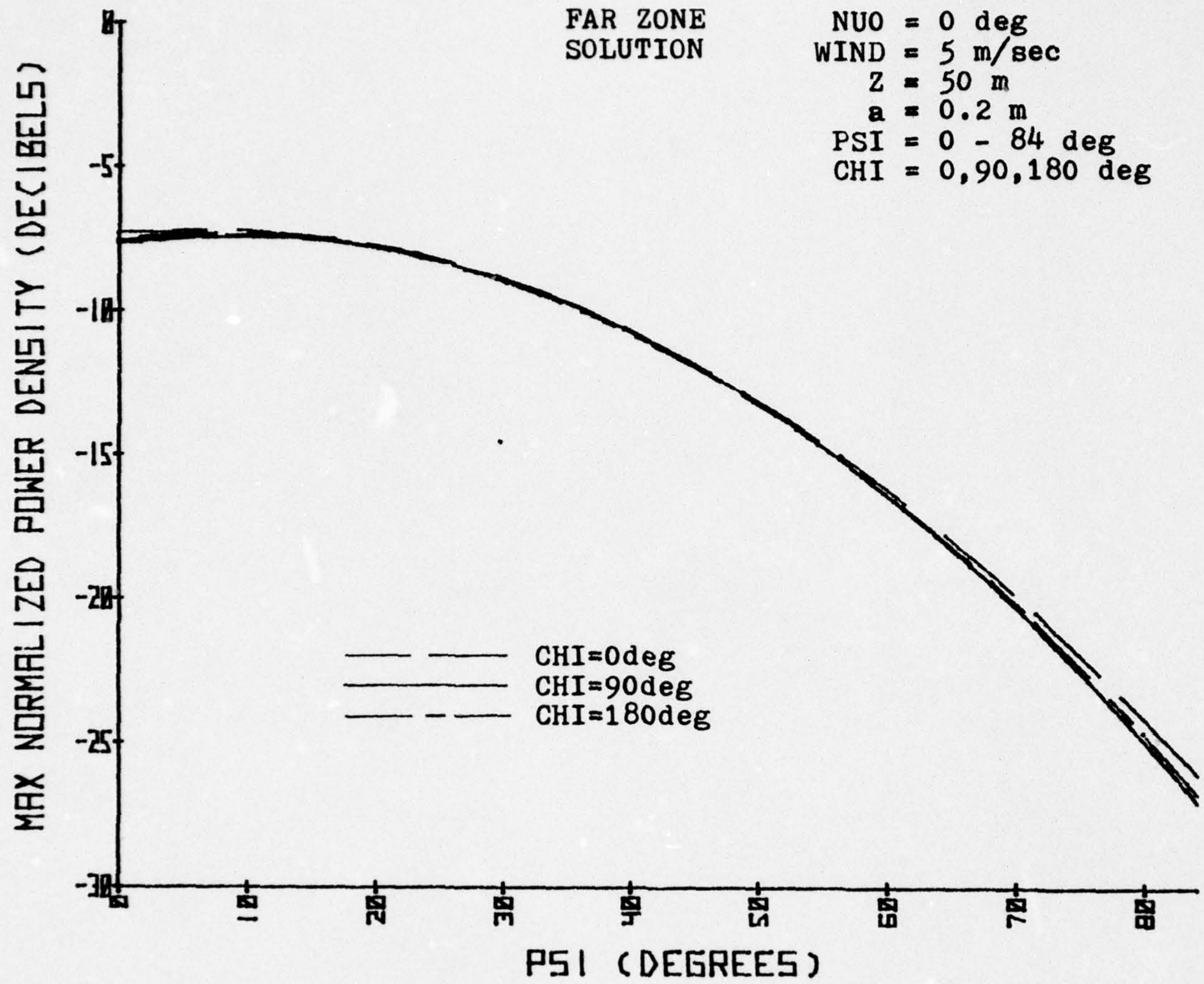
FAR ZONE
SOLUTION
NUO = 0 deg
WIND = 5 m/sec
Z = 50 m
a = 0.2 m
PSI = 0 - 84 deg
CHI = 0,90,180 deg
CHI=0deg
CHI=90deg
CHI=180deg
MAX NORMALIZED POWER DENSITY (DECIBELS)
0
-5
-10
-15
-20
-25
-30
0
10
20
30
40
50
60
70
80
PSI (DEGREES)

Figure 24

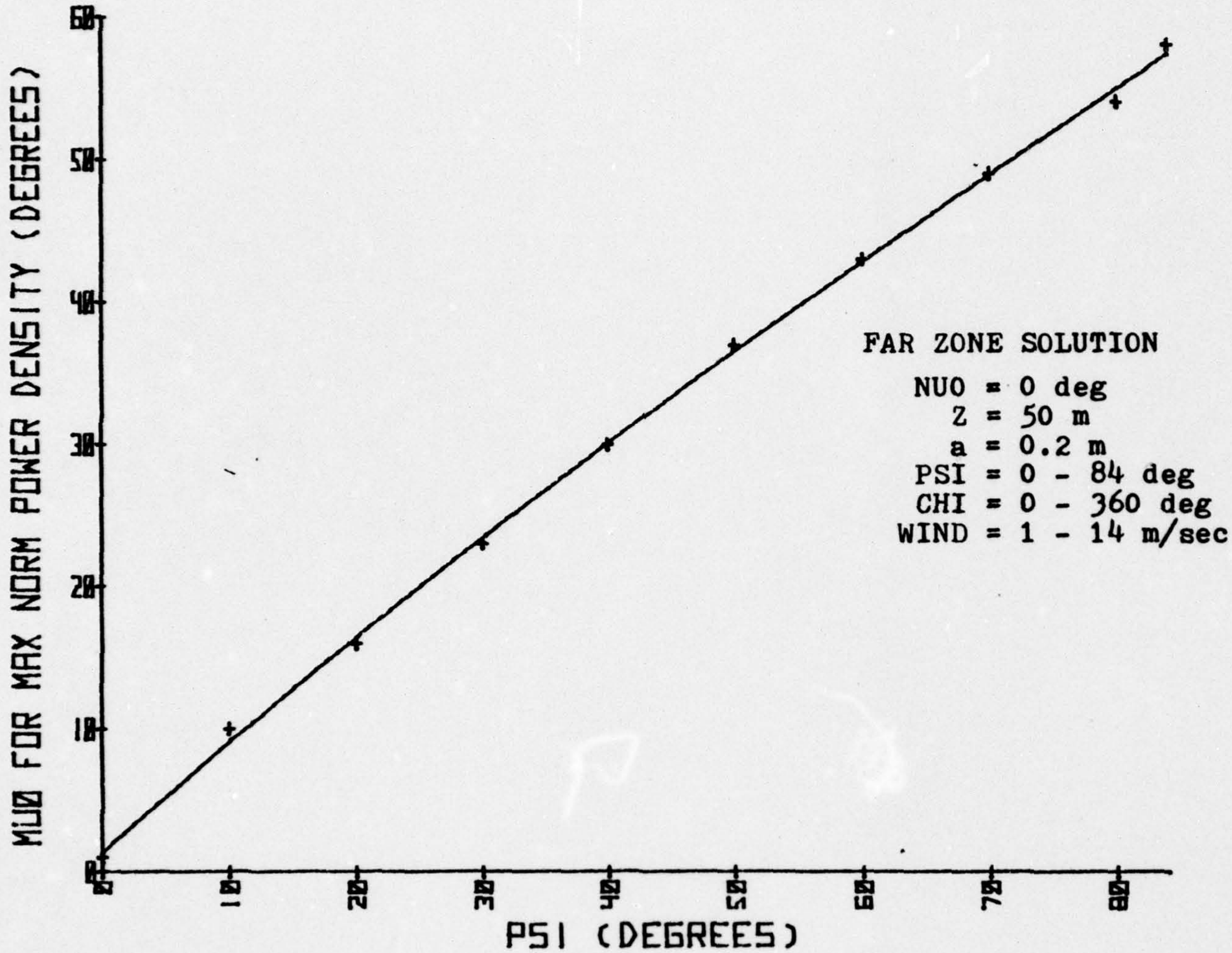
MUØ FOR MAX NORM POWER DENSITY (DEGREES)
PSI (DEGREES)
0
10
20
30
40
50
60
70
80
FAR ZONE SOLUTION
NUO = 0 deg
Z = 50 m
a = 0.2 m
PSI = 0 - 84 deg
CHI = 0 - 360 deg
WIND = 1 - 14 m/sec

Figure 25

APPENDIX B

COMPUTER PROGRAM USAGE

To use the computer programs listed following this Appendix, first compute the ratio of the depth of the point of observation below the ocean surface to the beam radius at the surface facet, Z/a. Use the Near Zone program for $Z/a \leq 100$ and the Far Zone program for $Z/a > 100$. The Near Zone program may be used for any value of Z/a, but a slight computation time and computer storage increase will result.

The only other basic requirement is the selection of eight input variables. The variables are listed below along with the line from the respective program in which they appear.

VARIABLE	NEAR ZONE	FAR ZONE
Depth, Z (m)	470	440
Beam radius, RAD (m)	480	450
Angle Nu_0, NUORUN (deg)	490	480
Backward scattering coefficient, BS	560	530
Absorption coefficient, AC (m^{-1})	570	540
Beam incidence angle, PSIRUN (deg)	630	590
Wind direction, CHI (rad)	680	640
Wind velocity, W (m/sec)	710	670

Z, RAD, NUORUN, BS and AC are direct program inputs

made on the indicated lines. PSI, CHI and W are selected from DATA statements 430 and 440 in the Near Zone program and 420 and 430 in the Far Zone program. The variable locations in DATA statements were used for multiple variations of the parameters in a slightly different form of the program than presented which is easily set up with DO LOOPS. The entry variables may also be varied in this same manner.

Both programs must be combined with the common package of subroutines that are listed following the basic program listings.

The cutput from both listed programs appear on the next two pages.

NEAR ZONE SOLUTION DEPTH= 10.00 M DTF= 0.37845 WIND=14.0 M/SEC
PSI=40.0 DEG RAD= 0.2 M VALID=1
NUO= 0.0 DEG CHI= 0.0 DEG INVALID=0

MUO	ALPHA	B	WI	WR	T	JACOB	PSLOPE	PRATIO	PWRDEN	MUO	VALIDITY	XI	ETA
15	0.0	29.93	69.93	44.93	0.2599	0.5512	1.7628E-01	8.5223E-05	-20.69	15	0	0.0	2.7
16	0.0	28.32	68.32	44.32	0.2869	0.4609	2.3785E-01	1.3573E-04	-18.67	16	0	0.0	2.6
17	0.0	26.66	66.66	43.66	0.3143	0.3841	3.1509E-01	2.1025E-04	-16.77	17	1	0.0	2.4
18	0.0	24.92	64.92	42.92	0.3420	0.3186	4.1207E-01	3.1866E-04	-14.96	18	1	0.0	2.2
19	0.0	23.11	63.11	42.11	0.3698	0.2624	5.3529E-01	4.7685E-04	-13.22	19	1	0.0	2.0
20	0.0	21.23	61.23	41.23	0.3975	0.2143	6.9461E-01	7.0772E-04	-11.50	20	1	0.0	1.8
21	0.0	19.26	59.26	40.26	0.4250	0.1730	9.0404E-01	1.0475E-03	-9.80	21	1	0.0	1.7
22	0.0	17.20	57.20	39.20	0.4521	0.1376	1.1812E 00	1.5486E-03	-8.10	22	1	0.0	1.5
23	0.0	15.04	55.04	38.04	0.4788	0.1073	1.5449E 00	2.2807E-03	-6.42	23	1	0.0	1.3
24	0.0	12.78	52.78	36.78	0.5048	0.0814	2.0097E 00	3.3303E-03	-4.78	24	1	0.0	1.1
25	0.0	10.41	50.41	35.41	0.5300	0.0592	2.5767E 00	4.7751E-03	-3.21	25	1	0.0	0.9
26	0.0	7.92	47.92	33.92	0.5542	0.0403	3.2231E 00	6.6605E-03	-1.76	26	1	0.0	0.7
27	0.0	5.32	45.32	32.32	0.5775	0.0242	3.8914E 00	8.9460E-03	-0.48	27	1	0.0	0.4
28	0.0	2.58	42.58	30.58	0.5995	0.0105	4.4854E 00	1.1450E-02	0.59	28	1	0.0	0.2
29	0.0	-0.28	39.72	28.71	0.6202	0.0010	4.8795E 00	1.3807E-02	1.40	29	1	0.0	0.0
30	0.0	-3.30	36.70	26.70	0.6395	0.0109	4.9488E 00	1.5517E-02	1.91	30	1	0.0	0.3
31	0.0	-6.44	33.56	24.56	0.6573	0.0192	4.6105E 00	1.6067E-02	2.04	31	1	0.0	0.5
32	0.0	-9.72	30.28	22.28	0.6735	0.0262	3.8757E 00	1.4895E-02	1.73	32	1	0.0	0.8
33	0.0	-13.14	26.86	19.86	0.6880	0.0323	2.8715E 00	1.2234E-02	0.88	33	1	0.0	1.1
34	0.0	-16.69	23.31	17.31	0.7008	0.0376	1.8156E 00	8.5815E-03	-0.66	34	1	0.0	1.4
35	0.0	-20.37	19.63	14.63	0.7117	0.0422	9.3345E-01	4.9045E-03	-3.09	35	1	0.0	1.8
36	0.0	-24.15	15.85	11.85	0.7206	0.0464	3.5898E-01	2.1022E-03	-6.77	36	1	0.0	2.1
37	0.0	-28.02	11.98	8.98	0.7277	0.0503	8.4646E-02	5.5445E-04	-12.56	37	0	0.0	2.5
38	0.0	-31.97	8.03	6.03	0.7328	0.0540	1.7671E-03	1.3010E-05	-28.86	38	0	0.0	3.0
39	0.0	-35.97	4.03	3.03	0.7359	0.0578	-6.2004E-03	5.1563E-05	-22.88	39	0	0.0	3.5

FAR ZONE SOLUTION DEPTH= 50.00 M DTF= 0.01121 WIND=14.0 M/SEC
PSI=40.0 DEG R3I= 0.2 M VALID=1
NUO= 0.0 DEG CHI= 0.0 DEG INVALID=0

MUO	ALPHA	B	WI	WR	T	JACOB	DAREA	PSLOPE	PRATIO	PWRDEN	MUC	VALIDITY	XI	ETA
15	0.0	29.93	69.93	44.93	0.2599	0.5512	2.2846E-04	1.7628E-01	7.9106E-08	-37.04	15	0	0.0	2.7
16	0.0	28.32	68.32	44.32	0.2869	0.4609	2.1142E-04	2.3785E-01	1.2603E-07	-35.02	16	0	0.0	2.6
17	0.0	26.66	66.66	43.66	0.3143	0.3841	1.9628E-04	3.1509E-01	1.9531E-07	-33.11	17	1	0.0	2.4
18	0.0	24.92	64.92	42.92	0.3420	0.3186	1.8170E-04	4.1207E-01	2.9471E-07	-31.33	18	1	0.0	2.2
19	0.0	23.11	63.11	42.11	0.3698	0.2624	1.6946E-04	5.3529E-01	4.4079E-07	-29.58	19	1	0.0	2.0
20	0.0	21.23	61.23	41.23	0.3975	0.2143	1.5934E-04	6.9461E-01	6.5843E-07	-27.84	20	1	0.0	1.8
21	0.0	19.26	59.26	40.26	0.4250	0.1730	1.4818E-04	9.0404E-01	9.6350E-07	-26.16	21	1	0.0	1.7
22	0.0	17.20	57.20	39.20	0.4521	0.1376	1.3892E-04	1.1812E 00	1.4326E-06	-24.46	22	1	0.0	1.5
23	0.0	15.04	55.04	38.04	0.4788	0.1073	1.3108E-04	1.5449E 00	2.1231E-06	-22.75	23	1	0.0	1.3
24	0.0	12.78	52.78	36.78	0.5048	0.0814	1.2235E-04	2.0097E 00	3.0907E-06	-21.13	24	1	0.0	1.1
25	0.0	10.41	50.41	35.41	0.5300	0.0592	1.1500E-04	2.5767E 00	4.4183E-06	-19.57	25	1	0.0	0.9
26	0.0	7.92	47.92	33.92	0.5542	0.0403	1.0876E-04	3.2231E 00	6.1994E-06	-18.10	26	1	0.0	0.7
27	0.0	5.32	45.32	32.32	0.5775	0.0242	1.0174E-04	3.8914E 00	8.2812E-06	-16.84	27	1	0.0	0.4
28	0.0	2.58	42.58	30.58	0.5995	0.0105	9.5727E-05	4.4854E 00	1.0598E-05	-15.77	28	1	0.0	0.2
29	0.0	-0.28	39.72	28.71	0.6202	0.0010	9.0677E-05	4.8795E 00	1.2862E-05	-14.93	29	1	0.0	0.0
30	0.0	-3.30	36.70	26.70	0.6395	0.0109	8.5383E-05	4.9488E 00	1.4460E-05	-14.42	30	1	0.0	0.3
31	0.0	-6.44	33.56	24.56	0.6573	0.0192	7.9832E-05	4.6105E 00	1.4817E-05	-14.31	31	1	0.0	0.5
32	0.0	-9.72	30.28	22.28	0.6735	0.0262	7.5110E-05	3.8757E 00	1.3788E-05	-14.63	32	1	0.0	0.8
33	0.0	-13.14	26.86	19.86	0.6880	0.0323	7.0705E-05	2.8715E 00	1.1324E-05	-15.48	33	1	0.0	1.1
34	0.0	-16.69	23.31	17.31	0.7008	0.0376	6.5718E-05	1.8156E 00	7.8486E-06	-17.07	34	1	0.0	1.4
35	0.0	-20.37	19.63	14.63	0.7117	0.0422	6.2218E-05	9.3345E-01	4.5155E-06	-19.47	35	1	0.0	1.8
36	0.0	-24.15	15.85	11.85	0.7206	0.0464	5.8849E-05	3.5898E-01	1.9475E-06	-23.13	36	1	0.0	2.1
37	0.0	-28.02	11.98	8.98	0.7277	0.0503	5.4906E-05	8.4646E-02	5.1006E-07	-28.94	37	C	0.0	2.5
38	0.0	-31.97	8.03	6.03	0.7328	0.0540	5.1929E-05	1.7671E-03	1.2050E-08	-45.21	38	C	0.0	3.0
39	0.0	-35.97	4.03	3.03	0.7359	0.0578	4.8740E-05	-6.2004E-03	4.7789E-08	-39.23	39	C	0.0	3.5

```
C       NEAR ZONE SOLUTION OF THE TIME-AVERAGE POWER PROBABILITY
C       DISTRIBUTION BELOW THE OCEAN OF A LASER BEAM INCIDENT ON SURFACE
C
C
C       NOMENCLATURE:
C
C            PSI=ANGLE OF INCIDENT BEAM WITH RESPECT TO VERTICAL AXIS
C            CHI=ANGLE OF WIND WITH RESPECT TO THE INCIDENT BEAM IN
C                THE XY-PLANE
C            ALPHA=ANGLE OF MAX WAVE SLOPE WITH RESPECT TO THE INCIDENT
C                  BEAM IN THE XY-PLANE
C            B=MAX SLOPE OF WAVE FACET
C            NU=NUO=ANGLE BETWEEN REFRACTED RAY PROJECTED ONTO XY-PLANE
C                   AND THE Y AXIS
C            MU=MUO=ANGLE BETWEEN REFRACTED RAY AND THE Z AXIS
C            Z=DEPTH BELOW OCEAN SURFACE (METERS)
C            RAD=INCIDENT RAY SPOT RADIUS AT WAVE FACET (MINOR AXIS OF
C                ELLIPSE WHEN PSI IS NON-ZERO)
C            BB=MAJOR AXIS OF SPOT INCIDENT ON WAVE FACET
C            W=WIND VELOCITY (M/SEC)
C            WI=RAY INCIDENCE ANGLE
C            WR=RAY REFRACTION ANGLE
C            CTF=DIFFUSE TRANSMITTANCE FUNCTION
C            BS=BACKWARD SCATTERING COEFFICIENT
C            AC=ABSORBTION COEFFICIENT
C            T=FRESNEL'S TRANSMITTANCE FUNCTION
C            AN=INDEX OF REFRACTION
C            PSLOPE=SLOPE PROBABILITY FUNCTION
C            DAREA=AREA INCREMENT
C            JACOB=JACOBIAN
C            PWRDEN=POWER DENSITY (DECIBELS)
C
        INTEGER VALID
        REAL NUO,JMUO,JACOB,MUO,NUORUN
        REAL MUU,MUL,NUU,NUL
        COMMON MUO,NUO,PSI,AN,PSIRUN,NUORUN,PI,Z,RAD,BB,JK
        DIMENSION W(4), CHI(3), NCHI(3), RG(4), JMUO(90), PWRDEN(90), PSIN
       1(10)
C
C       INPUT PARAMETERS FOR THIS RUN
C
        DATA W,CHI,NCHI/14.,10.,5.,1.,0.,1.5708,3.14159,0,90,180/
        DATA PSIN/0.,10.,20.,30.,40.,50.,60.,70.,80.,84./
        DATA ETA1,ETA2,XI1,XI2/.577350269,-.577350269,.577350269,-.5773502
       169/
        Z = 10.
        RAD = .2
```

```
      NUORUN = 0.
      NUO = NUORUN/57.2958
      AN = 1.33
      PI = 3.141592654
C
C     DIFFUSE TRANSMITTANCE FUNCTION (DTF)
C     REF 11: PG 65
      BS = .065
      AC = .044
      FK = SQRT(AC*(AC+2.*BS))
      DTF = FK/((AC+BS)*SINH(FK*Z)+FK*COSH(FK*Z))
C
C     PSI=40 DEG
      LM = 5
      PSIRUN = PSIN(5)
      PSI = PSIRUN/57.2958
      BE = RAD*(1./COS(PSI))
C
C     CHI=0 DEG
      L = 1
C
C     WIND=14 M/SEC
      I = 1
C
C     OUTPUT PRINTING INSTRUCTIONS
      WRITE (6,105) Z,DTF,W(I),PSIRUN,RAD,NUORUN,CHI(L)
  105 FORMAT (1H1,10X,'NEAR ZONE SOLUTION',5X,'DEPTH=',F6.2,' M',5X,
     1 'DTF=',F8.5,5X,'WIND=',F4.1,' M/SEC'/11X,'PSI=',F4.1,' DEG',11X,
     2 'RAD=',F5.1,' M',8X,'VALID=1'/11X,'NUO=',F4.1,' DEG',11X,'CHI=',
     3 F4.1,' DEG',7X,'INVALID=0'///)
C
      WRITE (6,110)
  110 FORMAT (1X,'MUO',2X,'ALPHA',4X,'B',7X,'WI',6X,'WR',6X,'T',5X,
     1 'JACOB',6X,'PSLOPE',5X,'PRATIO',5X,'PWRDEN',1X,
     2 'MUO',2X,'VALIDITY',2X,'XI',2X,'ETA'/)
C
C     MUO VARIED FROM 1 TO 90 DEG MAX FOR PSI LESS THAN OR EQUAL
C     TO 30 DEG, AND FROM 15 TO 90 DEG MAX FOR PSI GREATER THAN 30 DEG:
C     MUO IN RADIANS; JMUO IN DEGREES
C     REF 3: EQNS 50,54,55,82,83
C
      DO 115 J=1,90
      PWRDEN(J) = 0.
  115 CONTINUE
C
      IF (PSIRUN.GT.30.) GO TO 120
      INT = 1
      GO TO 125
```

```
  120 INT = 15
C
  125 DO 195 J=INT,90
      JMUO(J) = FLOAT(J)
      MUO = JMUO(J)/57.2958
      JK = J
      JJ = J-6
C
C     ALPHA,B,WI,WR ARE COMPUTED IN SUBROUTINE ANGLES:
      CALL ANGLES (ALPHA,B,WI,WR)
C     REFS 2,3&4
C
C     T=FRESNEL'S TRANSMITTANCE
C     REFS 9&10
      TPER = (2.*COS(WI)*SIN(WR)/SIN(WI+WR))**2
      TPAR = (2.*COS(WI)*SIN(WR)/SIN(WI+WR)*COS(WI-WR))**2
      T = (TPAR+TPER)/2.
C
C     JACOBIAN COMPUTED IN SUBROUTINE JACO
      CALL JACO (ALPHA,B,JACOB)
C     REF 3: EQNS 48-52
C
C     PSLOPE=SLOPE PROBIBILITY FUNCTION
C     REF 5: EQNS 5-9,12-18
      SIGC = SQRT(.003+1.92E-03*W(I))
      SIGU = SQRT(3.16E-03*W(I))
      C21 = .01-.0086*W(I)
      C03 = .04-.033*W(I)
      C40 = .4
      C22 = .12
      C04 = .23
      AP = ALPHA-CHI(L)
      ZXP = TAN(B)*SIN(AP)
      ZYP = TAN(B)*COS(AP)
      XI = ZXP/SIGC
      ETA = ZYP/SIGU
      FACT1 = (1./(2.*PI*SIGC*SIGU))*EXP(-.5*(XI**2+ETA**2))
      FACT2 = 1.-.5*C21*(XI**2-1.)*ETA-(1./6.)*C03*(ETA**3-3.*ETA)
      FACT3 = (1./24.)*C40*(XI**4-6.*XI**2+3.)+.25*C22*(XI**2-1.)*(ETA**
     12-1.)
      FACT4 = (1./24.)*C04*(ETA**4-6.*ETA**2+3.)
      PSLOPE = FACT1*(FACT2+FACT3+FACT4)
C
C     VALIDITY CHECK (VALID=1; INVALID=0) ON SLOPE PROBABILITY
      AXI = ABS(XI)
      AETA = ABS(ETA)
      VALID = 1
      IF ((AXI.GT.2.5).OR.(AETA.GT.2.5)) VALID=0
```

```
C
C     DETERMINE IF THE SURFACE PROJECTION OF THE POINT OF OBSERVATION
C     IS INSIDE OR OUTSIDE THE BEAM:
C     REF 3: EQNS 68-70,75-77
      Y1 = -(Z*TAN(MUO))/SQRT((TAN(NUO))**2+1.)
      IF (NUO.NE.0.) GO TO 130
      SUMCK1 = Y1+BB
      IF (SUMCK1.LT.0.) GO TO 135
      IF (SUMCK1.GE.0.) GO TO 170
  130 X1 = -(Z*TAN(MUO)*TAN(NUO))/SQRT((TAN(NUO))**2+1.)
      CTNU = COTAN(NUO)
      CA = CTNU*(X1*CTNU-Y1)
      CB = SQRT(BB**2*CTNU**2-(BB**2/RAD**2)*(Y1**2-BB**2+X1*CTNU*(X1*CT
     1NU-2.*Y1)))
      CC = CTNU**2+BB**2/RAD**2
      SUMCK2 = ABS(X1)-((CA-(SIN(NUO)/ABS(SIN(NUO)))*CB)/CC)
      IF (SUMCK2.GT.0.) GO TO 135
      IF (SUMCK2.LE.0.) GO TO 170
C
C     CALCULATION OF INTEGRATION LIMITS FOR THE SURFACE PROJECTION
C     OF THE POINT OF OBSERVATION OUTSIDE THE BEAM:
C     REF 3: EQNS 13,14,21-26,34-39,60-70
  135 IF (PSIRUN.EQ.0.) GO TO 155
C
C     OBLIQUE INCIDENCE, OUTSIDE BEAM:
      X1 = -(Z*TAN(MUO)*TAN(NUO))/SQRT(1.+TAN(NUO)**2)
      Y1 = -(Z*TAN(MUO))/SQRT(1.+TAN(NUO)**2)
C     INTERMEDIATE EQNS: ABX,AYS,BXAY
      ABX = (RAD**2)*(BB**2)*X1
      AYS = (RAD**2)*Y1*SQRT((BB**2)*(X1**2)-(RAD**2)*(BB**2)+(RAD**2)*(
     1Y1**2))
      BXAY = (BB**2)*(X1**2)+(RAD**2)*(Y1**2)
      X21 = (ABX-AYS)/BXAY
      X22 = (ABX+AYS)/BXAY
      IF (X1.LT.RAD) GO TO 140
      Y21 = BB*SQRT(1.-X21**2/RAD**2)
      Y22 = BB*SQRT(1.-X22**2/RAD**2)
      GO TO 145
  140 Y21 = -BB*SQRT(1.-X21**2/RAD**2)
      Y22 = -BB*SQRT(1.-X22**2/RAD**2)
  145 IF (NUO.NE.0.) GO TO 150
      X4 = 0.
      X5 = 0.
      Y4 = -BB
      Y5 = BB
      GO TO 165
  150 CTNU = COTAN(NUO)
      CA = CTNU*(X1*CTNU-Y1)
```

```
      CB = SQRT(BB**2*CTNU**2-(BB**2/RAD**2)*(Y1**2-BB**2+X1*CTNU*(X1*CT
     1NU-2.*Y1)))
      CC = CTNU**2+BB**2/RAD**2
      X4 = (CA-(SIN(NUO)/ABS(SIN(NUO)))*CB)/CC
      X5 = (CA+(SIN(NUO)/ABS(SIN(NUO)))*CB)/CC
      YY4 = BB*SQRT(1.-X4**2/RAD**2)
      Y4SG = (X4-X1)*CTNU+Y1
      Y4 = SIGN(YY4,Y4SG)
      YY5 = BB*SQRT(1.-X5**2/RAD**2)
      Y5SG = (X5-X1)*CTNU+Y1
      Y5 = SIGN(YY5,Y5SG)
      GO TO 165
C
C     NORMAL INCIDENCE, OUTSIDE BEAM:
  155 X1 = 0.
      Y1 = -Z*TAN(MUO)
      X21 = -(RAD*SQRT(Y1**2-RAD**2)/Y1)
      X22 = -X21
      Y21 = -RAD*SQRT(1.-X21**2/RAD**2)
      Y22 = -RAD*SQRT(1.-X22**2/RAD**2)
      IF (NUO.NE.0.) GO TO 160
      X4 = 0.
      X5 = 0.
      Y4 = -RAD
      Y5 = RAD
      GO TO 165
  160 CTNU = COTAN(NUO)
      CNA = -Y1*CTNU
      CNB = SQRT(RAD**2*CTNU**2-Y1**2+RAD**2)
      CNC = CTNU**2+1.
      X4 = (CNA-(SIN(NUO)/ABS(SIN(NUO)))*CNB)/CNC
      X5 = (CNA+(SIN(NUO)/ABS(SIN(NUO)))*CNB)/CNC
      YY4 = BB*SQRT(1.-X4**2/RAD**2)
      Y4SGN = X4*CTNU+Y1
      Y4 = SIGN(YY4,Y4SGN)
      YY5 = BB*SQRT(1.-X5**2/RAD**2)
      Y5SGN = X5*CTNU+Y1
      Y5 = SIGN(YY5,Y5SGN)
  165 B1 = SQRT((Y4-Y1)**2+(X4-X1)**2)
      B2 = SQRT((Y5-Y1)**2+(X5-X1)**2)
      DNU1 = ARCOS((Y1*(Y1-Y21)+X1*(X1-X21))/SQRT((X1**2+Y1**2)*((Y1-Y21
     1)**2+(X1-X21)**2)))
      DNU2 = ARCOS((Y1*(Y1-Y22)+X1*(X1-X22))/SQRT((X1**2+Y1**2)*((Y1-Y22
     1)**2+(X1-X22)**2)))
      MU1 = ATAN(B2/Z)
      MU2 = ATAN(B1/Z)
      NU1 = NUO+DNU1
      NU2 = NUO-DNU2
```

```
      GO TO 185
C
C     CALCULATION OF INTEGRATION LIMITS FOR THE SURFACE PROJECTION
C     OF THE POINT OF OBSERVATION INSIDE THE BEAM:
C     REF 3: EQNS 13,14,43-45,71-77
  170 X1 = -(Z*TAN(MUO)*TAN(NUO))/SQRT(1.+TAN(NUO)**2)
      Y1 = -(Z*TAN(MUO))/SQRT(1.+TAN(NUO)**2)
      IF ((NUO.EQ.0.).OR.(NUO.EQ.PI)) GO TO 175
      X6 = (COTAN(NUO)*(X1*COTAN(NUO)-Y1)+SQRT(BB**2*COTAN(NUO)**2-(BB**
     12/RAD**2)*(Y1-BB**2+X1*COTAN(NUO)*(X1*COTAN(NUO)-2.*Y1))))/(COTAN(
     2NUO)**2+BB**2/RAD**2)
      YY6 = BB*SQRT(1.-X6**2/RAD**2)
      Y6SG = Y1+(X6-X1)*COTAN(NUO)
      Y6 = SIGN(YY6,Y6SG)
      GO TO 180
  175 Y6 = 0.
  180 B3 = SQRT((Y6-Y1)**2+(X6-X1)**2)
      MUU = ATAN(B3/Z)
      MUL = 0.
      NUU = 2.*PI
      NUL = 0.
C
C     PRATIO=POWER DENSITY RATIO
C     COMPUTED USING A TWO-POINT GAUSS-LEGENDRE QUADRATURE
C     NUMERICAL INTEGRATION SCHEME
C     REF 3: EQN 53
C     REFS 14&15
C     CINT=CONSTANT DURING INTEGRATION
  185 CINT = T*COS(WI)*(1./COS(WR))*PSLOPE*TAN(B)*(1./COS(B))**2*(1./JAC
     1OB)*(((MUU-MUL)*(NUU-NUL))/4.)*CTF
      ETAMU1 = ((MUU-MUL)*ETA1+MUU+MUL)/2.
      ETAMU2 = ((MUU-MUL)*ETA2+MUU+MUL)/2.
      XINU1 = ((NUU-NUL)*XI1+NUU+NUL)/2.
      XINU2 = ((NUU-NUL)*XI2+NUU+NUL)/2.
      FXT1 = COS(ETAMU1)*COS(MUO)+SIN(ETAMU1)*SIN(MUO)*COS(ABS(XINU1-NUO
     1))
      FXT2 = COS(ETAMU1)*COS(MUO)+SIN(ETAMU1)*SIN(MUO)*COS(ABS(XINU2-NUO
     1))
      FXT3 = COS(ETAMU2)*COS(MUO)+SIN(ETAMU2)*SIN(MUO)*COS(ABS(XINU2-NUO
     1))
      FXT4 = COS(ETAMU2)*COS(MUO)+SIN(ETAMU2)*SIN(MUO)*COS(ABS(XINU1-NUO
     1))
      PRATIO = ABS(CINT*(FXT1+FXT2+FXT3+FXT4))
C
      PWRDEN(J) = 10.*ALOG10(PRATIO*Z**2)
C     REF 2: PGS 65-67; FIG 34
C
C     OUTPUT INSTRUCTIONS
```

```
C     CCNVERT ALPHA,B,WI,WR FROM RADIANS TO DEGREES
      RCEG = 57.2958
      ALPHAD = ALPHA*RDEG
      BD = B*RDEG
      WIC = WI*RDEG
      WRD = WR*RDEG
      WRITE (6,190) J,ALPHAD,BD,WIC,WRC,T,JACOB,PSLCPE,PRATIO,PWRDEN(J),
     1J,VALIC,AXI,AETA
  190 FCRMAT (1X,I2,1X,F7.2,1X,F7.2,1X,F7.2,1X,F7.2,1X,F7.4,1X,F7.4,1X,1
     1PE11.4,1X,1PE11.4,1X,0PF8.2,2X,I2,5X,I2,3X,F4.1,1X,F4.1)
C
C     LCCP EXIT FOR LOW SLOPE PROBABILITY
      IF ((PSLOPE.LT.1.E-20).AND.(PWRDEN(J).LT.PWRDEN(JJ)).AND.(J.GT.5))
     1 GC TO 200
  195 CCNTINUE
C
  200 CCNTINUE
      ENC
```

```
C        FAR ZONE SOLUTION OF THE TIME-AVERAGE POWER PROBABILITY
C        DISTRIBUTION BELOW THE OCEAN OF A LASER BEAM INCIDENT
C        ON THE SURFACE
C
C
C        NOMENCLATURE:
C
C             PSI=ANGLE OF INCIDENT BEAM WITH RESPECT TO VERTICAL AXIS
C             CHI=ANGLE OF WIND WITH RESPECT TO THE INCIDENT BEAM IN
C                 THE XY-PLANE
C             ALPHA=ANGLE OF MAX WAVE SLOPE WITH RESPECT TO THE INCIDENT
C                   BEAM IN THE XY-PLANE
C             B=MAX SLOPE OF WAVE FACET
C             NU=NUO=ANGLE BETWEEN REFRACTED RAY PROJECTED ONTO XY-PLANE
C                    AND THE Y AXIS
C             MU=MUO=ANGLE BETWEEN REFRACTED RAY AND THE Z AXIS
C             Z=DEPTH BELOW OCEAN SURFACE (METERS)
C             RAD=INCIDENT RAY SPOT RADIUS AT WAVE FACET (MINOR AXIS OF
C                 ELLIPSE WHEN PSI IS NON-ZERO)
C             BB=MAJOR AXIS OF SPOT INCIDENT ON WAVE FACET
C             W=WIND VELOCITY (M/SEC)
C             WI=RAY INCIDENCE ANGLE
C             WR=RAY REFRACTION ANGLE
C             DTF=DIFFUSE TRANSMITTANCE FUNCTION
C             BS=BACKWARD SCATTERING COEFFICIENT
C             AC=ABSORBTION COEFFICIENT
C             T=FRESNEL'S TRANSMITTANCE FUNCTION
C             AN=INDEX OF REFRACTION
C             PSLOPE=SLOPE PROBABILITY FUNCTION
C             DAREA=AREA INCREMENT
C             JACOB=JACOBIAN
C             PWRDEN=POWER DENSITY (DECIBELS)
C
C
         INTEGER VALID
         REAL NUO,JMUO,JACOB,MLO,NUORUN
         COMMON MUO,NUO,PSI,AN,PSIRUN,NUORUN,PI,Z,RAD,BB,JK
         DIMENSION W(3), CHI(3), NCHI(3), RG(4), JMUO(90), PWRDEN(90), PSIN
        1(10)
C
C        INPUT PARAMETERS:
         DATA W,CHI,NCHI/14.,10.,5.,0.,1.5708,3.14159,0,90,180/
         DATA PSIN/0.,10.,20.,30.,40.,50.,60.,70.,80.,84./
         Z = 50.
         RAD = .2
         PI = 3.141592654
         AN = 1.33
         NUORUN = 0.
```

```
      NUO = NUORUN/57.2958
C
C     DIFFUSE TRANSMITTANCE FUNCTION (DTF)
C     REF 11: PG 65
      BS = .065
      AC = .044
      FK = SQRT(AC*(AC+2.*BS))
      DTF = FK/((AC+BS)*SINH(FK*Z)+FK*COSH(FK*Z))
C
C     PSI = 40 DEG
      PSIRUN = PSIN(5)
      PSI = PSIRUN/57.2958
      BE = RAD*(1./COS(PSI))
C
C     WIND DIRECTION CHI = 0 DEG
      L = 1
C
C     WIND=14 M/SEC
      I = 1
C
C     OUTPUT PRINTING INSTRUCTIONS
C
      WRITE (6,105) Z,DTF,W(I),PSIRUN,RAD,NUORUN,CHI(L)
  105 FORMAT (1H1,10X,'FAR ZONE SOLUTION',5X,'DEPTH=',F6.2,' M',5X,
     1 'DTF=',F8.5,5X,'WIND=',F4.1,' M/SEC'/11X,'PSI=',F4.1,' DEG',10X,
     2 'RAD=',F5.1,' M',8X,'VALID=1'/11X,'NUO=',F4.1,' DEG',10X,'CHI=',
     3 F4.1,' DEG',7X,'INVALID=0'///)
C
      WRITE (6,110)
  110 FORMAT (1X,'MUO',2X,'ALPHA',5X,'B',6X,'WI',6X,'WR',6X,'T',5X,
     1 'JACOB',5X,'DAREA',6X,'PSLOPE',7X,'PRATIC',5X,'PWRDEN',1X,
     2 'MUO',2X,'VALIDITY',1X,'XI',3X,'ETA'/)
C
C     MUO VARIED FROM 1 TO 90 DEG MAX FOR PSI LESS THAN OR EQUAL
C     TO 30 DEG, AND FROM 15 TO 90 DEG MAX FOR PSI GREATER THAN 30 DEG:
C     MUO IN RADIANS; JMUO IN DEGREES
C     REF 3: EQNS 50,54,55,82,83
C
      DO 115 J=1,90
      PWRDEN(J) = 0.
  115 CONTINUE
C
      IF (PSIRUN.GT.30.) GO TO 120
      INT = 1
      GO TO 125
  120 INT = 15
C
  125 DO 135 J=INT,90
```

```
      JMLO(J) = FLOAT(J)
      MLC = JMUO(J)/57.2958
      JK = J
      JL = J-6
C
C     ALPHA,B,WI,WR ARE COMPUTED IN SUBROUTINE ANGLES:
C     REFS 2,3&4
      CALL ANGLES (ALPHA,B,WI,WR)
C
C     T=FRESNEL'S TRANSMITTANCE
C     REFS 9&10
      TPER = (2.*COS(WI)*SIN(WR)/SIN(WI+WR))**2
      TPAR = (2.*COS(WI)*SIN(WR)/SIN(WI+WR)*COS(WI-WR))**2
      T = (TPAR+TPER)/2.
C
C     JACOBIAN COMPUTED IN SUBROUTINE JACO
C     REF 3: EQNS 48-52
      CALL JACO (ALPHA,B,JACOB)
C
C     AREA INCREMENT (DAREA) COMPUTED IN SUBROUTINE AREA
C     REF 3: EQNS 13,14,21-24,38,39,79,80
      CALL AREA (DAREA)
C
C     FSLCPE=SLOPE PROBIBILITY FUNCTION
C     REF 5: EQNS 5-9,12-18
      SIGC = SQRT(.003+1.92E-03*W(I))
      SIGU = SQRT(3.16E-03*W(I))
      C21 = .01-.0086*W(I)
      C03 = .04-.033*W(I)
      C40 = .4
      C22 = .12
      CC4 = .23
      AP = ALFHA-CHI(L)
      ZXP = TAN(B)*SIN(AP)
      ZYP = TAN(B)*COS(AP)
      XI = ZXP/SIGC
      ETA = ZYP/SIGU
      FACT1 = (1./(2.*PI*SIGC*SIGU))*EXP(-.5*(XI**2+ETA**2))
      FACT2 = 1.-.5*C21*(XI**2-1.)*ETA-(1./6.)*C03*(ETA**3-3.*ETA)
      FACT3 = (1./24.)*C40*(XI**4-6.*XI**2+3.)+.25*C22*(XI**2-1.)*(ETA**
     12-1.)
      FACT4 = (1./24.)*C04*(ETA**4-6.*ETA**2+3.)
      FSLCPE = FACT1*(FACT2+FACT3+FACT4)
C
C     VALIDITY CHECK (VALID=1; INVALIC=0) ON SLCPE PROBABILITY
      AXI = ABS(XI)
      AETA = ABS(ETA)
      VALID = 1
```

```
      IF ((AXI.GT.2.5).OR.(AETA.GT.2.5)) VALID=0
C
C     PRATIO=POWER DENSITY RATIO
C     REFS 2,3&4
      PRATIO = ABS(DTF*T*TAN(B)*((1./CCS(B))**2)*COS(WI)*(1./CCS(WR))*PS
     1LCPE*CAREA/JACOB)
C
      PWRDEN(J) = 10.*ALOG10(PRATIO*Z**2)
C     REF 2: PGS 65-67; FIG 34
C
C     CUTPUT INSTRUCTIONS
C     CCNVERT ALPHA,B,WI,WR FROM RADIANS TO DEGREES
      RDEG = 57.2958
      ALPHAD = ALPHA*RDEG
      BD = B*RDEG
      WID = WI*RDEG
      WRD = WR*RDEG
      WRITE (6,130) J,ALPHAD,BD,WID,WRD,T,JACOB,CAREA,PSLCPE,PRATIO,PWRD
     1EN(J),J,VALID,AXI,AETA
  130 FCRMAT (1X,I2,1X,F7.2,1X,F7.2,1X,F7.2,1X,F7.2,1X,F7.4,1X,F7.4,1X,1
     1PE11.4,1X,1PE11.4,1X,1PE11.4,1X,0PF8.2,2X,I2,5X,I2,3X,F4.1,1X,F4.1
     2)
C
C     LCCP EXIT FOR LOW SLOPE PROBABILITY
      IF ((PSLCPE.LT.1.E-40).AND.(PWRDEN(J).LT.PWRDEN(JJ)).AND.(J.GT.5))
     1 GC TO 140
  135 CCNTINUE
C
  140 CCNTINUE
      END
```

```
      SUBROUTINE ANGLES (ALPHA,B,WI,WR)
C
C     SUBROUTINE ANGLES SOLVES FOR ALPHA,B,WI&WR GIVEN PSI,NUO,MUO&AN
C
      EXTERNAL FINDAB,FINDB
      REAL NUO,MUO,NUORUN
      COMMON MUO,NUO,PSI,AN,PSIRUN,NUORUN,PI,Z,RAD,BB,JK
      DIMENSION Q(2), Y(1)
      IF (PSIRUN.EQ.0.) GO TO 230
      IF (NUORUN.EQ.0.) GO TO 215
C
C     SOLUTION FOR PSI&NUO NON-ZERO:
C     ALPHA & B FOR A GIVEN MUO & NUO ARE OBTAINED BY SOLVING
C     SIMULTANEOUS NON-LINEAR EQNS 82&83 OF REF 3 USING IBM SOURCE
C     LIB SUBROUTINE (NLNSYS)
C
C     FIRST ESTABLISH INITIAL GUESS FOR NLNSYS
      IF ((JK.EQ.1).OR.((JK.EQ.15).AND.(PSIRUN.GT.30.))) GO TO 205
      Q(1) = ALPHA
      Q(2) = B
      GO TO 210
  205 Q(1) = .1
      Q(2) = .1
  210 CALL NLNSYS (2,10,4,ISING,1,FINDAB,Q)
      ALPHA = Q(1)
      B = Q(2)
      WI = ARCOS(COS(PSI)*COS(B)-SIN(PSI)*COS(ALPHA)*SIN(B))
      WR = ARCOS((1./AN)*SQRT(COS(WI)**2+AN**2-1.))
      GO TO 235
C
C     SOLUTION FOR PSI NON-ZERO & NUO=0.0:
  215 ALPHA = 0.
C     B SOLVED FROM NON-LINEAR EQN 82 OF REF 3 USING IBM SOURCE LIB
C     SUBROUTINE (NLNSYS);  FIRST ESTABLISH INITIAL  B GUESS
      IF ((JK.EQ.1).OR.((JK.EQ.15).AND.(PSIRUN.GT.30.))) GO TO 220
      Y(1) = B
      GO TO 225
  220 Y(1) = .1
  225 CALL NLNSYS (1,10,4,ISING,1,FINDB,Y)
      B = Y(1)
      WI = ARCOS(COS(PSI)*COS(B)-SIN(PSI)*SIN(B))
      WR = ARCOS((1./AN)*SQRT(COS(WI)**2+AN**2-1.))
      GO TO 235
C
C     SOLUTION FOR PSI=0.0:
  230 ALPHA = NUO
      B = ATAN((AN*SIN(MUO))/(AN*COS(MUO)-1.))
      WI = B
```

```
      WR = ARSIN((1./AN)*SIN(B))
C
  235 RETURN
      END
```

```
      SUBROUTINE FINDAB (Q,F,K)
C
C     SUBROUTINE USED BY NLNSYS FOR COMPUTING THE (ALPHA&B) PAIR
C
C                Q(1)=ALPHA
C                Q(2)=B
C
      REAL MUO,NUO,NUORUN
      COMMON MUO,NUO,PSI,AN,PSIRUN,NUORUN,PI,Z,RAC,BB,JK
      DIMENSION Q(2)
      IF (K.EQ.1) GO TO 305
      GO TO 310
C
  305 F = -COS(MUO)+(1./AN)*(COS(PSI)+(SIN(PSI)*COS(Q(1))*SIN(Q(2))-COS(
     1PSI)*COS(Q(2))+SQRT((SIN(PSI)*COS(Q(1))*SIN(Q(2))-COS(PSI)*COS(Q(2
     2)))**2+AN**2-1.))*COS(Q(2)))
      GO TO 315
C
  310 F = -COTAN(NUO)+COTAN(Q(1))-SIN(PSI)/(SIN(Q(1))*SIN(Q(2))*(SIN(PSI
     1)*COS(Q(1))*SIN(Q(2))-COS(PSI)*COS(Q(2))+SQRT((SIN(PSI)*COS(Q(1))*
     2SIN(Q(2))-COS(PSI)*COS(Q(2)))**2+AN**2-1.)))
C
  315 RETURN
      END
```

```
      SLBROUTINE FINDB (Y,F,K)
C
C     SLBROUTINE FINDB USED BY NLNSYS FCR COMPUTING B;   B=Y(1)
C
      REAL MLO,NUO,NUORUN
      CCMMON MUO,NUO,PSI,AN,PSIRUN,NUORUN,PI,Z,RAC,BB,JK
      DIMENSICN Y(1)
      SPSI = SIN(PSI)
      CFSI = COS(PSI)
C
      F = -COS(MUO)+(1./AN)*(CPSI+(SPSI*SIN(Y(1))-CPSI*COS(Y(1))+SQRT((S
     1PSI*SIN(Y(1))-CPSI*COS(Y(1)))**2+AN**2-1))*COS(Y(1)))
C
      RETURN
      END
```

```
      SUBROUTINE JACO (ALPHA,B,JACOB)
C
C     SUBROUTINE JACO COMPUTES THE JACOBIAN FOR NORMAL & OBLIQUE
C     INCIDENCE.
C
      REAL JACOB,MUO,NUO,NUORUN
      COMMON MUO,NUO,PSI,AN,PSIRUN,NUORUN,PI,Z,RAC,BB,JK
      IF (PSIRUN.EQ.0.) GO TO 505
C
C     JACOBIAN FOR OBLIQUE INCIDENCE:
      AKK = SQRT((SIN(PSI)*COS(ALPHA)*SIN(B)-COS(PSI)*COS(B))**2+AN**2-1
     1.)
      SK = (SIN(PSI)*COS(ALPHA)*SIN(B)-COS(PSI)*COS(B))+AKK
      DKDA = ((SIN(PSI)*SIN(ALPHA)*SIN(B)*(COS(PSI)*COS(B)-SIN(PSI)*COS(
     1ALPHA)*SIN(B)))/AKK)-SIN(PSI)*SIN(ALPHA)*SIN(B)
      DKDB = (((SIN(PSI)*COS(ALPHA)*SIN(B)-COS(PSI)*COS(B))*(SIN(PSI)*CO
     1S(ALPHA)*COS(B)+COS(PSI)*SIN(B)))/AKK)+(SIN(PSI)*COS(ALPHA)*COS(B)
     2+COS(PSI)*SIN(B))
      D = ((SK*SIN(ALPHA)*SIN(B))**2+(SK*COS(ALPHA)*SIN(B)-SIN(PSI))**2)
     1*SQRT(AN**2-(COS(PSI)+SK*COS(B))**2)
      JACOB = ABS((1./D)*((COS(B)*SIN(ALPHA)*SIN(PSI)*DKDA)*(DKDB*SIN(B)
     1+SK*COS(B))+(DKDB*COS(B)-SK*SIN(B))*((SK*SIN(B))**2-(SIN(PSI)*SIN(
     2B))*(DKDA*SIN(ALPHA)+SK*COS(ALPHA)))))
      GO TO 510
C
C     JACOBIAN FOR NORMAL INCIDENCE:
  505 AK = -COS(B)+SQRT(COS(B)**2+AN**2-1.)
      DKDB = SIN(B)*(1.-(COS(B)/SQRT(COS(B)**2+AN**2-1.)))
      JACOB = ABS((1./SQRT(AN**2-(1.+AK*COS(B))**2))*(DKDB*COS(B)-AK*SIN
     1(B)))
C
  510 RETURN
      END
```

```
      SUBROUTINE AREA (DAREA)
C
C     SUBROUTINE AREA COMPUTES THE AREA INCREMENT (DAREA) FOR
C     NORMAL & OBLIQUE INCIDENCE.
C
      REAL MUO,NUO,NUORUN
      COMMON MUO,NUO,PSI,AN,PSIRUN,NUORUN,PI,Z,RAD,BB,JK
      CALL ERRSET (251,500,-1,1)
      IF (PSIRUN.EQ.0.) GO TO 625
C
C     DAREA FOR OBLIQUE INCIDENCE:
      X1 = -(Z*TAN(MUO)*TAN(NUO))/SQRT(1.+TAN(NUO)**2)
      Y1 = -(Z*TAN(MUO))/SQRT(1.+TAN(NUO)**2)
C     INTERMEDIATE EQNS: ABX,AYS,BXAY
      ABX = (RAD**2)*(BB**2)*X1
      AYS = (RAD**2)*Y1*SQRT((BB**2)*(X1**2)-(RAD**2)*(BB**2)+(RAD**2)*(
     1Y1**2))
      BXAY = (BB**2)*(X1**2)+(RAD**2)*(Y1**2)
      X21 = (ABX-AYS)/BXAY
      X22 = (ABX+AYS)/BXAY
      IF (X1.LT.RAD) GO TO 605
      Y21 = BB*SQRT(1.-X21**2/RAD**2)
      Y22 = BB*SQRT(1.-X22**2/RAD**2)
      GO TO 610
  605 Y21 = -BB*SQRT(1.-X21**2/RAD**2)
      Y22 = -BB*SQRT(1.-X22**2/RAD**2)
  610 IF (NUO.NE.0.) GO TO 615
      X4 = 0.
      X5 = 0.
      Y4 = -BB
      Y5 = BB
      GO TO 620
  615 CTNU = COTAN(NUO)
      CA = CTNU*(X1*CTNU-Y1)
      CB = SQRT(BB**2*CTNU**2-(BB**2/RAD**2)*(Y1**2-BB**2+X1*CTNU*(X1*CT
     1NU-2.*Y1)))
      CC = CTNU**2+BB**2/RAD**2
      X4 = (CA-(SIN(NUO)/ABS(SIN(NUO)))*CB)/CC
      X5 = (CA+(SIN(NUO)/ABS(SIN(NUO)))*CB)/CC
      YY4 = BB*SQRT(1.-X4**2/RAD**2)
      Y4SG = (X4-X1)*CTNU+Y1
      Y4 = SIGN(YY4,Y4SG)
      YY5 = BB*SQRT(1.-X5**2/RAD**2)
      Y5SG = (X5-X1)*CTNU+Y1
      Y5 = SIGN(YY5,Y5SG)
  620 C1 = SQRT((Y5-Y1)**2+(X5-X1)**2)/Z
      C2 = SQRT((Y4-Y1)**2+(X4-X1)**2)/Z
      C3 = (Y1*(Y1-Y21)+X1*(X1-X21))/SQRT((X1**2+Y1**2)*((Y1-Y21)**2+(X1
```

```
     1-X21)**2))
      C4 = (Y1*(Y1-Y22)+X1*(X1-X22))/SQRT((X1**2+Y1**2)*((Y1-Y21)**2+(X1
     1-X21)**2))
      IF (C3.GT.1.0) C3 = 1.0
      IF (C4.GT.1.0) C4 = 1.0
      CAREA = ((PI/4.)*(ATAN(C1)-ATAN(C2)))*(ARCOS(C3)+ARCOS(C4))
      GC TO 640
C
C     CAREA FCR NORMAL INCIDENCE:
  625 X1 = 0.
      Y1 = -Z*TAN(MUO)
      X21 = -(RAD*Y1*SQRT(Y1**2-RAD**2))/Y1**2
      X22 = -X21
      Y21 = -RAD*SQRT(1.-X21**2/RAD**2)
      Y22 = -RAD*SQRT(1.-X22**2/RAD**2)
      IF (NUO.NE.0.) GO TO 630
      X4 = 0.
      X5 = 0.
      Y4 = -RAD
      Y5 = RAD
      GC TO 635
  63C CTNU = COTAN(NUO)
      CNA = -Y1*CTNU
      CNB = SCRT(ABS(RAD**2*CTNU**2-Y1**2+RAD**2))
      CNC = CTNU**2+1.
      X4 = (CNA-(SIN(NUO)/ABS(SIN(NUO)))*CNB)/CNC
      X5 = (CNA+(SIN(NUO)/ABS(SIN(NUO)))*CNB)/CNC
      YY4 = BB*SQRT(1.-X4**2/RAD**2)
      Y4SGN = X4*CTNU+Y1
      Y4 = SIGN(YY4,Y4SGN)
      YY5 = BB*SQRT(1.-X5**2/RAD**2)
      Y5SGN = X5*CTNU+Y1
      Y5 = SIGN(YY5,Y5SGN)
  635 C1 = SQRT((Y5-Y1)**2+(X5-X1)**2)/Z
      C2 = SQRT((Y4-Y1)**2+(X4-X1)**2)/Z
      C3 = (Y1*(Y1-Y21)+X1*(X1-X21))/SQRT((X1**2+Y1**2)*((Y1-Y21)**2+(X1
     1-X21)**2))
      C4 = (Y1*(Y1-Y22)+X1*(X1-X22))/SQRT((X1**2+Y1**2)*((Y1-Y21)**2+(X1
     1-X21)**2))
      IF (C3.GT.1.0) C3 = 1.0
      IF (C4.GT.1.0) C4 = 1.0
      CAREA = ((PI/4.)*(ATAN(C1)-ATAN(C2)))*(ARCCS(C3)+ARCCS(C4))
C
  64C RETURN
      END
```

```
      SUBROUTINE NLNSYS(N,MAXIT,NUMSIG,ISING,IPRINT,EVALUT,X)           NLNS1430
C                                                                       NLNS1440
C     NLNSYS SOLVES A SYSTEM OF SIMULTANEOUS NON-LINEAR EQUATIONS
C     NLNSYS IS FROM THE IBM SYSTEM 360 SUBROUTINE LIBRARY
C
      DIMENSION X(1)                                                    NLNS1450
      INTEGER CONVRG,TALLY,PCNTER                                       NLNS1460
      COMMON/SSSS/ISUB(19),COE(20,21),PCNTER(20,20)                     NLNS1470
      EXTERNAL EVALUT                                                   NLNS1480
      DIMENSION TEMP(20),PART(20)                                       NLNS1490
C                                                                       NLNS1500
      CONVRG=1                                                          NLNS1510
C         INITIALIZE CONVERGENCE AND TOLERANCE DETERMINERS.             NLNS1520
      ISING=0                                                           NLNS1530
      RELCON=10.**(-NUMSIG)                                             NLNS1540
C         ITERATION LOOP.                                               NLNS1550
      DO 55 M=1,MAXIT                                                   NLNS1560
C         PROGRAM WILL PRINT OUT SUCCESSIVE APPROXIMATIONS OF X IF      NLNS1570
C         IPRINT IS 0.                                                  NLNS1580
      IF (IPRINT.EQ.0) WRITE (6,1000) M,(X(I),I=1,N)                    NLNS1590
 1000 FORMAT(1X,12HON ITERATION,I4,17HTHE X ESTIMATE IS,5F15.7/7F15.7/  NLNS1600
     1           7F15.7///)                                             NLNS1610
C         INITIALIZE FIRST ROW OF ARRAY WHICH ENABLES INDEXING TO PIVOT NLNS1620
C         THROUGH THE VARIABLES WITHOUT INTERCHANGING ROWS OR COLUMNS.  NLNS1630
      DO 5 J=1,N                                                        NLNS1640
    5 PCNTER(1,J)=J                                                     NLNS1650
C         ONE K FOR EACH EQUATION.                                      NLNS1660
      DO 40 K=1,N                                                       NLNS1670
C         IF K IS GREATER THAN 1 BACK-SUBSTITUTION IS NECESSARY.        NLNS1680
      IF (K.GT.1) CALL BAKSUB(K,N,X)                                    NLNS1690
      CALL EVALUT(X,F,K)                                                NLNS1700
      FACTOR=.001                                                       NLNS1710
    7 TALLY=0                                                           NLNS1720
      DO 10 I=K,N                                                       NLNS1730
      ITEMP=PCNTER(K,I)                                                 NLNS1740
      HOLD=X(ITEMP)                                                     NLNS1750
C         GET INCREMENT TO OBTAIN ITEMP'TH PARTIAL.                     NLNS1760
      H=FACTOR*HOLD                                                     NLNS1770
      IF (H.EQ.0.) H=.001                                               NLNS1780
      X(ITEMP)=HOLD+H                                                   NLNS1790
C         IF K IS GREATER THAN 1, A NEW X(ITEMP) VALUE WILL AFFECT X'S  NLNS1800
C         WHICH ARE EXPRESSED IN TERMS OF IT AS A RESULT OF PREVIOUS    NLNS1810
C         EQUATION STEPS.                                               NLNS1820
      IF (K.GT.1) CALL BAKSUB(K,N,X)                                    NLNS1830
      CALL EVALUT(X,FPLUS,K)                                            NLNS1840
C         GET ITEMP'TH PARTIAL.                                         NLNS1850
      PART(ITEMP)=(FPLUS-F)/H                                           NLNS1860
      X(ITEMP)=HOLD                                                     NLNS1870
```

```
C         IF PARTIAL IS TOO SMALL, INCREASE TALLY.'                     NLNS1880
      IF(ABS(PART(ITEMP)).EQ.0) GO TO 9                                 NLNS1890
      IF(ABS(F/PART(ITEMP)).GT.1.0E20) TALLY=TALLY+1                    NLNS1891
      GO TO 10                                                          NLNS1892
    9 TALLY=TALLY+1                                                     NLNS1893
   10 CONTINUE                                                          NLNS1910
      IF (TALLY.LE.(N-K)) GO TO 15                                      NLNS1920
      FACTOR=FACTOR*10.0                                                NLNS1930
C         IF SURFACE IS TOO FLAT, THE SINGULARITY INDICATOR IS SET TO   NLNS1940
C         ZERO AND RETURN IS EXECUTED.                                  NLNS1950
      IF (FACTOR.GT..5) GO TO 65                                        NLNS1960
      GO TO 7                                                           NLNS1970
   15 IF(K.LT.N) GO TO 20                                               NLNS1980
C         IF LAST PARTIAL IS ZERO, A SINGULARITY IS INDICATED AND A     NLNS1990
C         RETURN EXECUTED.                                              NLNS2000
      IF (ABS(PART(ITEMP)).EQ.0.) GO TO 65                              NLNS2010
      COE(K,N+1)=0                                                      NLNS2020
      KMAX=ITEMP                                                        NLNS2030
      GO TO 40                                                          NLNS2040
   20 KMAX=PONTER(K,K)                                                  NLNS2050
      DERMAX=ABS(PART(KMAX))                                            NLNS2060
      KPLUS=K+1                                                         NLNS2070
C         GET INDEX FOR LARGEST PARTIAL IN K'TH EQUATION.               NLNS2080
      DO 30 I=KPLUS,N                                                   NLNS2090
      JSUB=PONTER(K,I)                                                  NLNS2100
      TEST=ABS(PART(JSUB))                                              NLNS2110
      IF (TEST.LT.DERMAX) GO TO 25                                      NLNS2120
      DERMAX=TEST                                                       NLNS2130
C         DEFINE PIVOT TO SWIVEL ABOUT THE VARIABLE WITH MAXIMUM PARTIAL NLNS2140
C         WHEN WE GET TO THE NEXT EQUATION.                             NLNS2150
      PONTER(KPLUS,I)=KMAX                                              NLNS2160
C         IF THIS PARTIAL IS BIGGER, WE HAVE A NEW MAXIMUM.             NLNS2170
      KMAX=JSUB                                                         NLNS2180
      GO TO 30                                                          NLNS2190
   25 PONTER(KPLUS,I)=JSUB                                              NLNS2200
   30 CONTINUE                                                          NLNS2210
C         IF THAT PARTIAL IS 0, INDICATE A SINGULARITY AND RETURN.      NLNS2220
      IF (ABS(PART(KMAX)).EQ.0) GO TO 65                                NLNS2230
      ISUB(K)=KMAX                                                      NLNS2240
      COE(K,N+1)=0                                                      NLNS2250
      DO 35 J=KPLUS,N                                                   NLNS2260
      JSUB=PONTER(KPLUS,J)                                              NLNS2270
C         SAVE THESE CONSTANTS FOR FUTURE USE.                          NLNS2280
      COE(K,JSUB)=-PART(JSUB)/PART(KMAX)                                NLNS2290
C         GET PART OF EXPRESSION FOR THE NEW X(KMAX) VALUE              NLNS2300
   35 COE(K,N+1)=COE(K,N+1)+PART(JSUB)*X(JSUB)                          NLNS2310
   40 COE(K,N+1)=(COE(K,N+1)-F)/PART(KMAX)+X(KMAX)                      NLNS2320
C         IF N IS 1, WE HAVE OUR SOLUTION IN THE NEXT STEP WITHOUT ANY  NLNS2330
```

```
C         BACK-SUBSTITUTING.                                             NLNS2340
      X(KMAX)=COE(N,N+1)                                                 NLNS2350
C         FOR N GREATER THAN 1, WE PERFORM A FINAL BACK-SUBSTITUTICN TO  NLNS2360
C         GET OUR NEW X-VECTOR.                                          NLNS2370
      IF (N.GT.1) CALL BAKSUB(N,N,X)                                     NLNS2380
      IF (M.EQ.1) GO TO 50                                               NLNS2390
      DC 43 I=1,N                                                        NLNS2400
C         TEST FOR CONVERGENCE.                                          NLNS2410
      IF (ABS((TEMP(I)-X(I))/X(I)).GT.RELCON) GO TO 45                   NLNS2420
   43 CCNTINUE                                                           NLNS2430
      CCNVRG=CONVRG+1                                                    NLNS2440
C         IF IT CCNVERGES, RETURN WITH LAST VECTCR.                      NLNS2450
      IF (CONVRG.GE.3) GO TO 60                                          NLNS2460
      GC TO 50                                                           NLNS2470
   45 CCNVRG=1                                                           NLNS2480
C         SAVE CURRENT X-VECTOR FOR TESTING WITH NEXT X-VECTOR.          NLNS2490
   50 DC 55 I=1,N                                                        NLNS2500
   55 TEMP(I)=X(I)                                                       NLNS2510
C         IF M IS THE ITERATION LIMIT, RETURN.                           NLNS2520
      GC TO 70                                                           NLNS2530
   6C MAXIT=M                                                            NLNS2540
      GC TO 70                                                           NLNS2550
   65 ISING=1                                                            NLNS2560
   70 RETURN                                                             NLNS2570
      ENC                                                                NLNS2580
```

```
      SUBROUTINE BAKSUB(K,N,X)                                          BKSB2600
C
C        THIS SUBROUTINE BACK-SUBSTITUTES OR UPDATES VARIABLES WHICH AREBKSB2610
C        FUNCTIONS OF CURRENT X ENTRY VALUES.                           BKSB2620
C     BAKSUB IS PART OF THE NLNSYS ROUTINE.
C
      DIMENSION X(1)                                                    BKSB2630
      INTEGER PONTER                                                    BKSB2640
      COMMON/SSSS/ISUB(19),COE(20,21),PONTER(20,20)                     BKSB2650
C                                                                       BKSB2660
      DO 10 KMM=2,K                                                     BKSB2670
      KM=K+2-KMM                                                        BKSB2680
      KMAX=ISUB(KM-1)                                                   BKSB2690
      X(KMAX)=0.                                                        BKSB2700
      DO 5 J=KM,N                                                       BKSB2710
      JSUB=PONTER(KM,J)                                                 BKSB2720
C        SEE (3) FOR THE EXPRESSION FOR X(KMAX).                        BKSB2730
    5 X(KMAX)=X(KMAX)+COE(KM-1,JSUB)*X(JSUB)                            BKSB2740
   10 X(KMAX)=X(KMAX)+COE(KM-1,N+1)                                     BKSB2750
      RETURN                                                            BKSB2760
      END                                                               BKSB2770
```

LIST OF REFERENCES

1. Karp, S., " Optical Communications Between Underwater and Above Surface (Satellite) Terminals", *IEEE Transactions on Communications*, v. 24, p. 66-81, January 1976.

2. Antenna Laboratory, The Ohio State University Research Foundation, Report 1675-3, *The Power Probability Distribution Below the Ocean Surface of Diffuse and Collimated Incident Optical Energy*, by J. P. Swennen, 21 December 1964.

3. Antenna Laboratory, The Ohio State University Research Foundation, Report 2170-1, *Power Density Probability Distribution Below the Ocean Surface of a Beam of Collimated Optical Radiation Obliquely Incident on the Surface*, by J. P. Swennen, 31 March 1966.

4. Swennen, J. P., " Time-Average Power-Density Distribution Below the Ocean Surface of a Beam of Collimated Optical Radiation Incident on the Surface", *Journal of the Optical Society of America*, v. 50, p. 224-229, February 1966.

5. Cox, C. S. and Munk, W. H., " Measurement of the Roughness of the Sea Surface from Photographs of the Sun's Glitter", *Journal of the Optical Society of America*, v. 44, p. 838-850, November 1954.

6. Groen, P., *The Waters of the Sea*, p. 122-185, Van Nostrand Reinhold, 1969.

7. New York University Department of Meteorology and

Oceanography Geophysical Sciences Laboratory Report 63-15, The Interpretation of Wave Spectra in Terms of the Wind Profile Instead of the Wind Measured at a Constant Height, by W. J. Pierson, Jr., 1963.

8. Hill, M. N., The Sea-Ideas and Observations on Progress in the Study of the Seas, p. 567-589,664-699, Wiley, 1962.

9. Born, M. and Wolf, E., Principles of Optics, p. 36-51, Pergamon Press, 1975.

10. Fowles, G. R., Introduction to Modern Optics, p. 33-60, Holt, Rinehart and Winston, 1968.

11. Duntley, S. Q., " The Optical Properties of Diffusing Materials", Journal of the Optical Society of America, v. 32, p. 61-70, February 1942.

12. Tyler, J. E., " Scattering Properties of Distilled and Natural Waters", Limnology and Oceanography, v. 6, p. 451, October 1961.

13. Duntley, S. Q., " Light in the Sea", Journal of the Optical Society of America, v. 53, p. 214-233, February 1963.

14. Carnahan, B., Luther, H. A. and Wilkes, J. O., Applied Numerical Methods, p. 101-116, Wiley, 1969.

15. Gerald, C. F., Applied Numerical Analysis, p. 59-72, Addison-Wesley, 1973.

16. Preisendorfer, R. W., Hydrologic Optics, v. 1-6, U. S. Department of Commerce(NOAA), 1976.

17. Prettyman, C. E. and Cermak, M. D., " The Variation of the Rough Ocean Surface and its Effects on an Incident Laser Beam", IEEE Transactions on Geoscience Electronics, v. 7, p. 235-243, October 1969.

18. Bucher, E. A., " Propagation Models for Optical Communication Through Fog and Clouds", _Proceedings of the National Electronics Conference_, v. 29, p. 180-185, 1974.

INITIAL DISTRIBUTION LIST

		No. Copies
1.	Defense Documentation Center Cameron Station Alexandria, Virgina 22314	2
2.	Library, Code 0142 Naval Postgraduate School Monterey, california 93940	2
3.	Department Chairman, Code 67 Department of Aeronautics Naval Postgraduate School Monterey, california 93940	1
4.	Professor D. J. Collins, Code 67Co Department of Aeronautics Naval Postgraduate School Monterey, california 93940	1
5.	Naval Ocean Systems Center, Code 725 Attn: LT Giannaris, USN 271 Catalina Blvd. San Diego, California 92152	1
6.	LT Michael J. Milchanowski, USN Air Force Weapons Laboratory Kirtland AFB New Mexico 87115	1